AMERICAN SOCIETY FOR MICROBIOLOGY | Molecular and Cellular Biology®

RESEARCH ARTICLE

IRC3 Regulates Mitochondrial Translation in Response to Metabolic Cues in *Saccharomyces cerevisiae*

Jaswinder Kaur,[a] Kaustuv Datta[a]

[a]Department of Genetics, University of Delhi, New Delhi, India

ABSTRACT Mitochondrial oxidative phosphorylation (OXPHOS) enzymes have a dual genetic origin. Mechanisms regulating the expression of nucleus-encoded OXPHOS subunits in response to metabolic cues (glucose versus glycerol) are well understood, while the regulation of mitochondrially encoded OXPHOS subunits is poorly defined. Here, we show that *IRC3*, a DEAD/H box helicase gene, previously implicated in mitochondrial DNA maintenance, is central to integrating metabolic cues with mitochondrial translation. Irc3 associates with mitochondrial small ribosomal subunits in cells consistent with its role in regulating translation elongation based on the Arg8^m reporter system. *IRC3*-deleted cells retained mitochondrial DNA despite a growth defect on glycerol plates. Glucose-grown $\Delta irc3\rho^+$ and *irc3* temperature-sensitive cells at 37°C have reduced translation rates from the majority of mRNAs. In contrast, when galactose was the carbon source, a reduction in mitochondrial translation was observed predominantly from Cox1 mRNA in $\Delta irc3\rho^+$ cells but no defect was observed in *irc3* temperature-sensitive cells, at 37°C. In support of a model whereby *IRC3* responds to metabolic cues to regulate mitochondrial translation, $\Delta irc3$ suppressor strains isolated for restoration of growth on glycerol medium restore mitochondrial protein synthesis differentially in the presence of glucose versus glycerol.

KEYWORDS mitochondria, OXPHOS, RNA helicase, metabolic cues, translation

Mitochondria, which are best known as the powerhouse of the cell, require coordinated gene expression of two spatially distinct genetic materials. Mitochondria are essential for an organism's viability and normal physiology, and any disruption in its functioning leads to a myriad of cellular defects, including cancer (1–3). *Saccharomyces cerevisiae* has been an invaluable system for deciphering mitochondrial function, due to its ability to survive without respiration as well as mitochondrial DNA (mtDNA), permitting the characterization of mutants that impair mitochondrial functioning. In *Saccharomyces cerevisiae*, mtDNA encodes eight proteins, seven of which are transmembrane proteins that are essential components of oxidative phosphorylation (OXPHOS) machinery and one, soluble protein Var1, that is an essential component of mitochondrial small ribosomal subunits. In addition to these eight protein coding genes, mtDNA also encodes rRNAs (15S and 21S) and a complete set of tRNAs required for gene expression. The remainder of the proteins that make up the OXPHOS subunits, factors required for mitochondrial transcription and translation, including mitochondrial ribosomal proteins, are encoded by the nuclear genome, which is translated in the cytosol and imported into the mitochondria (4).

Translation of mitochondrial mRNA, in addition to general translation factors such as Tuf1 (EF-Tu) and Mef1 and Mef2 (EF-G), require membrane-bound mRNA-specific translation activators (5–11). In the absence of either Shine-Dalgarno sequences or a 5′ cap on mitochondrial transcripts, these mRNA-specific translation activators recognize the 5′ untranslated region (UTR) of mRNA to localize them to the mitochondrial inner membrane, where they aid in the loading of membrane-bound ribosomes to initiate mitochondrial translation (12–18). In fact, each mitochondrial mRNA has its specific set of translation activators (19, 20). Interestingly, altered levels or activities of these translation activators are thought to allow

Citation Kaur J, Datta K. 2021. *IRC3* regulates mitochondrial translation in response to metabolic cues in *Saccharomyces cerevisiae*. Mol Cell Biol 41:e00233-21. https://doi.org/10.1128/MCB.00233-21.

Address correspondence to Kaustuv Datta, kdatta@south.du.ac.in.

Received 20 May 2021
Returned for modification 7 July 2021
Accepted 11 August 2021
Accepted manuscript posted online 16 August 2021
Published 26 October 2021

yeast cells to sense metabolic cues. For yeast cells, transfer from fermentable to nonfermentable growth leads to enhanced OXPHOS expression and activity. This is brought about by enhanced expression of nucleus-encoded OXPHOS subunits and mitochondrial mRNA-specific translation factors, which upregulates translation of mitochondrially encoded OXPHOS subunits (21–23). Another way mitochondrial translation responds to alteration in metabolic cues is by using different mitochondrial translation factors under different conditions. For example, the translation from *COX1* mRNA is controlled by *PET309*, *MSS51*, and *MAM33* (24–29). Mam33 is required for the translation of Cox1 at the basal level in glucose-grown yeast cells along with Pet309p and Mss51p. However, its function is dispensable in cells adapted for growth in glycerol, where *COX1* mRNA translation is regulated primarily by Mss51p and Pet309p (29).

In addition to translation factors, optimal mitochondrial gene expression requires the essential function of RNA helicase, among other accessory proteins. They regulate every aspect of mitochondrial RNA metabolism, including RNA splicing, mRNA turnover/surveillance, translation, and ribosome biogenesis (30–32). RNA helicases utilize energy released from ATP hydrolysis to promote rearrangements required by nascent RNA molecules to arrive at a mature structure (33–35). These mature structures are achieved by the action of helicases to unwind double-stranded RNA (dsRNA), anneal single-stranded RNA (ssRNA), modify RNA-DNA hybrids, and displace proteins bound to RNA (36–38). In *Saccharomyces cerevisiae*, the nuclear genome encodes four mitochondrial helicases which belong to the SFII family of NTP-dependent remodelers containing a DExH/D motif that regulates different aspects of mitochondrial function. *MSS116* has been shown to play a role in transcription, mRNA splicing, and translation (39–42), while *MRH4* and *SUV3* are known to be involved in ribosome biogenesis and RNA editing/turnover, respectively (43–46). The fourth mitochondrial helicase gene, *IRC3*, has been implicated in mtDNA recombination and repair (47, 48). However, these studies were carried out in strains deleted for *IRC3*, in which the loss of mtDNA could be either due to a direct role of Irc3 in regulating mtDNA recombination/repair or to an indirect consequence of Irc3's role in an essential process involving RNA molecules, such as transcription and translation.

In the present study, we have shown that *IRC3* is a central regulator of mitochondrial translation. Interestingly, Irc3p regulates mitochondrial translation distinctly in cells grown in a carbon source that maintains OXPHOS at basal (glucose) versus elevated (galactose/glycerol) levels. Glucose-grown Δ*irc3*ρ^+ cells were defective for overall mitochondrial protein synthesis in addition to reducing the accumulation of mitochondrial transcripts. In contrast, glucose-grown cells harboring *irc3* temperature-sensitive mutants have reduced rates of translation, without having any consequence on the levels of mRNA transcripts or assembled mitochondrial ribosomal subunits, when shifted to the nonpermissive temperature. Interestingly, for galactose-grown Δ*irc3*ρ^+ cells and cells harboring *irc3* temperature-sensitive mutants, a reduction in mitochondrial translation from Cox1 mRNA was observed in Δ*irc3*ρ^+ cells but not in cells harboring *irc3* temperature-sensitive mutants at the nonpermissive temperature. Consistent with a role in translation regulation, Irc3 cofractionates with small ribosomal subunits when cells are grown in either glucose or glycerol. Importantly, we have shown that *IRC3* is required for translation elongation in glucose-grown cells. Consistent with a hypothesis whereby the mechanisms of action and targets of *IRC3* are different under conditions that maintain mitochondrial function at a basal level and those that have higher mitochondrial function, we were able to isolate Δ*irc3*ρ^+suppressor strains that restored mitochondrial translation to different degrees when the cells were grown in glucose versus glycerol.

RESULTS

***IRC3* is essential for normal respiratory growth.** To determine whether *IRC3* regulates an essential mitochondrial function in cells, we sporulated a heterozygous diploid Δ*irc3* strain generated in the lab. Although the numbers of colonies formed on glucose plates in freshly germinated Δ*irc3* or *IRC3* spores were similar, Δ*irc3* spores formed two types of colonies which could be differentiated based on colony size. On glycerol plates, a lower number of Δ*irc3* spores formed CFUs than did *IRC3* spores, although the colony sizes were comparable. In fact, the numbers of large colonies formed on glucose plates were

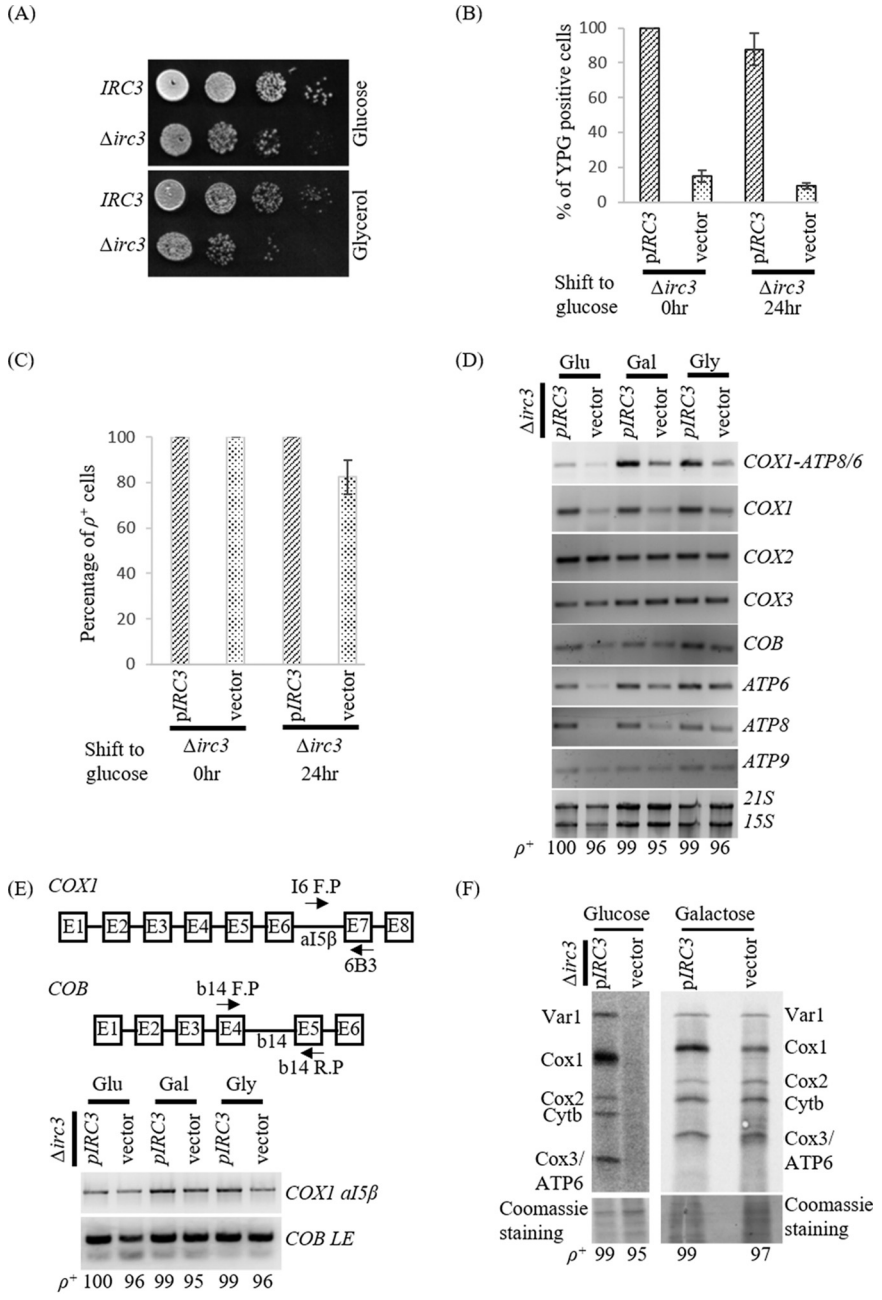

FIG 1 Loss of growth on glycerol precedes loss of mtDNA in Δ*irc3*ρ^+ cells due to aberrant gene expression. (A) Tenfold serial dilutions of freshly germinated spores of wild-type and Δ*irc3* cells spotted on glucose or glycerol plates are shown. (B) Percentages of viable Δ*irc3* progeny cells expressing either an episomal copy of *IRC3* or empty vector that can utilize glycerol as the sole carbon source at the indicated time points upon subculturing in glucose. Three independent colonies of wild-type and Δ*irc3* cells were used to calculate the % YPG-positive cells. Five independent replicates of this experiment were performed. (C) Percentages of mtDNA present in Δ*irc3* progeny expressing either an episomal copy of *IRC3* or vector at the indicated time after subculture in glucose. Three independent colonies of wild-type and Δ*irc3* cells were used to calculate the % ρ^+ cells. Five independent replicates of this experiment were performed. (D) Transcript levels of mitochondrial genes were assayed in Δ*irc3* cells expressing either an episomal copy of *IRC3* or vector grown in glucose, galactose, and glycerol. 21S rRNA and 15S rRNA levels were detected by EtBr staining. Samples were normalized for total RNA. Multiple independent biological and technical replicates were carried out, and representative images are shown. (E) Upper panel, schematic representation of exons and introns in the *COX1* and *COB* transcripts. Primers subsequently used to determine the splice variant in *COX1* and *COB* transcripts are indicated by arrows. Lower panel, levels of transcripts of pre-mRNA of *COX1* (*COX1 aI5*β, product of primers I6 F.P and 6B3) and *COB* ligated exon (Cytb LE, b14F.P, and b14R.P). (F) Mitochondrial protein synthesis was measured in Δ*irc3* cells

(Continued on next page)

equivalent to the numbers of colonies formed on glycerol plates (Fig. 1A). To minimize the effect of an unlinked mutation on the inability of Δ*irc3* spores to utilize glycerol, Δ*irc3/IRC3* cells episomally expressing wild-type *IRC3* linked to *URA3* were sporulated. The Δ*irc3* spores episomally expressing the *IRC3* allele linked to *URA3* were backcrossed six times as described in Material and Methods. The reduced ability of freshly generated Δ*irc3* cells (colonies obtained on 5FOAD [0.67% yeast nitrogen base without amino acids containing 0.1% 5-fluoro-orotic acid and 2% glucose]) to utilize glycerol as the sole carbon source was a fraction of the total viable cells in comparison to that of Δ*irc3* cells ectopically expressing *IRC3* when cultured either in glucose, galactose, or glycerol (see Fig. S1A in the supplemental material). This indicated that ectopic expression of *IRC3* was able to complement the glycerol growth defect. All further experiments were carried out using this six-time-backcrossed strain (KDY 1146). Furthermore, the percentage of total viable cells that were able to utilize glycerol as the sole carbon source was estimated in Δ*irc3* cells expressing either wild-type *IRC3* or vector upon subculturing in glucose for 0 h and 24 h. We observed that 10% of progeny cells were competent for cellular respiration in a population of Δ*irc3* cells in comparison to 90% of wild-type cells upon subculturing in glucose or glycerol for 24 h (Fig. 1B; Fig. S1B). Thus, taken together, this indicates that *IRC3* is essential for optimal mitochondrial function. Mitochondrial DNA integrity has been reported to be compromised in yeast cells defective for essential processes related to mitochondrial DNA maintenance and gene expression. Measurement of timing of the loss of ability to utilize growth on glycerol versus loss of mtDNA in mutant cells is often indicative of the primary role played by the wild-type copy of the mutant gene product (43, 49, 50). Thus, we determined the status of mtDNA (*rho* or ρ) in a population of haploid Δ*irc3* cells containing either empty vector or episomally expressing *IRC3* upon subculturing in glucose medium for 0 h and 24 h at 30°C. Aliquots of cells at each time point were crossed with wild-type ρ^0 cells of the opposite mating type. The ability of the diploids generated to utilize glycerol is indicative of the presence of mitochondrial DNA in the parental haploid Δ*irc3* cells. Approximately 90 to 100% of cells episomally expressing a wild-type copy of *IRC3* retained mitochondrial DNA upon subculturing in glucose. In Δ*irc3* cells, approximately 85% of the cells retained mtDNA upon subculturing in glucose for 24 h (Fig. 1C). However, further incubation of Δ*irc3* cells led to loss of mitochondrial DNA, such that only 20% of cells retained mitochondrial DNA upon subculturing in glucose for 72 h (Fig. S1C). Further, to quantify mtDNA and analyze its stability in Δ*irc3* cells expressing either wild-type *IRC3* or vector, upon subculturing them in glucose for 0 h and 24 h, we measured the mtDNA copy number with respect to the nuclear DNA (nDNA) copy number as described in Material and Methods. Ratios of mtDNA to nDNA were similar in cells deleted for *IRC3* and in wild-type cells even after subculturing in glucose for 24 h (Fig. S1D). Thus, all subsequent experiments using Δ*irc3*ρ^+ cells were carried out under culture conditions such that cells retained mitochondrial DNA. Taken together, our results indicate that loss of growth on glycerol precedes loss of mitochondrial DNA in Δ*irc3* cells. This is suggestive of a defect in an essential process within the mitochondria in Δ*irc3* cells such as those linked to mitochondrial gene expression as the primary cause of loss of cellular respiration and loss of mitochondrial DNA as a secondary consequence. Similar phenotypes have been reported for numerous mutant genes that are defective in mitochondrial gene expression (43, 49, 50).

***IRC3* is essential for mitochondrial gene expression.** IRC3 is a putative helicase of the SFII family, a majority of which have been known to act on RNA molecules (51, 52). Thus, *IRC3* could potentially be involved in transcription, splicing, RNA maturation and turnover, ribosome assembly, or translation to regulate mitochondrial gene expression.

FIG 1 Legend (Continued)
expressing either an episomal copy of *IRC3* or vector cultured in either glucose or galactose at 30°C. Labeling reaction was carried out by incorporation of ^{35}S-labeled methionine and cysteine in the presence of cycloheximide to inhibit cytosolic protein synthesis at 30°C for 30 min. Mitochondria from labeled cells were isolated, and equivalent amounts of mitochondrial proteins were separated on a 17.5% SDS-PAGE gel and transferred to a nitrocellulose membrane. Radiolabeled proteins were visualized by phosphorimaging. Shown at the bottom is a Coomassie blue-stained gel of radiolabeled mitochondrial protein extracts. Percentages of mitochondrial DNA present in the respective strains are indicated at the bottom of the gels in panels D to F.

Mitochondrial transcript levels were examined in Δ*irc3*ρ^+ cells grown in either glucose, galactose, or glycerol by performing reverse transcriptase PCR as described in Materials and Methods. Transcript levels of *COX1*, *ATP6*, and *ATP8* were reduced in Δ*irc3*ρ^+ cells in comparison to wild-type cells, although steady-state levels of *COB*, *COX2*, *COX3*, and *ATP9* mRNA remained relatively unchanged (Fig. 1D). These observations were consistent irrespective of the carbon sources used for cell culture (Fig. 1D). To determine whether the reduced transcript levels in cells deleted for *IRC3* is a consequence of improper intron splicing, we analyzed Δ*irc3*ρ^+ cells for efficient splicing of *COX1* and *COB* transcripts. To check the accumulation of transcripts where the a15β intron is retained in cDNAs synthesized from *COX1* transcripts, primers used for reverse transcriptase PCR were designed between a15β and exon7 (I6F.P and 6B3). To amplify the ligated exon from synthesized cDNA for *COB* transcripts, primers were designed from exonic regions upstream and downstream of b14 (b14F.P and b14R.P) introns (Fig. 1E, top). In comparison to wild-type cells, the levels of unspliced mRNA, i.e., *COX1 a15*β, did not accumulate in Δ*irc3*ρ^+ cells (Fig. 1E). The levels of *COB* ligated exon were similar to transcript levels of *COB* (Fig. 1E and D). In addition, we found that Δ*irc3* cells harboring intronless mtDNA led to glycerol growth defects similar to those in Δ*irc3* cells harboring wild-type mtDNA (Fig. S1E). These results are suggestive of a role for *IRC3* independent of regulating RNA splicing. The observed reduction in steady-state levels of *COX1*, *ATP8*, and *ATP6* could be due either to a defect in polycistronic transcript formation or in its subsequent processing. The *COX1*, *ATP8*, and *ATP6* genes are transcribed on a polycistronic RNA that undergoes processing at two unique maturation sites downstream of *COX1* 3′ UTR to yield an independent *ATP8/ATP6* transcript (53, 54). In order to test whether processing was defective, we analyzed the presence of polycistronic mRNA (*COX1-ATP8/ATP6*) in *IRC3* and Δ*irc3*ρ^+ cells using primers upstream and downstream of these maturation sites (Fig. S1F). We found a reduction in the polycistronic mRNA levels in Δ*irc3*ρ^+ cells compared to that in wild-type cells consistent with a defect in transcript formation rather than maturation (Fig. 1D).

To ascertain whether mitochondrial translation is also perturbed in Δ*irc3*ρ^+ cells, newly synthesized polypeptides were labeled in Δ*irc3*ρ^+ cells either episomally expressing *IRC3* or transformed with vector backbone after growth in glucose and galactose. Growth of cells in glucose leads to glucose repression, whereby expression of genes required for alternate carbon sources as well as mitochondrial oxidative phosphorylation is downregulated. However, growth in galactose does not repress genes required for either fermentation or cellular respiration and thus considered to be neutral for these pathways (55–57). *De novo* labeling of mitochondrial proteins in Δ*irc3*ρ^+ cells grown on glucose indicated a severe defect in incorporation of ^{35}S-labeled methionine and cysteine into newly synthesized proteins, in comparison to the wild type (Fig. 1F). In contrast, *de novo* labeling of mitochondrial proteins in Δ*irc3*ρ^+ cells grown in galactose led to reduced incorporation of ^{35}S-labeled methionine and cysteine into newly synthesized Cox1 polypeptides in comparison to wild-type cells (Fig. 1F). This indicates that Irc3p is pivotal for mitochondrial translation irrespective of the type of carbon source in which the cells are grown.

Within the mitochondria, transcription and translation are tightly coupled, presumably to make mitochondrial gene expression more efficient and faster (58–61). Thus, diminished accumulation of mRNA levels in Δ*irc3*ρ^+ cells could be indirect consequences of altered translation rates or *vice versa*.

***IRC3* is essential for mitochondrial translation during basal OXPHOS activity.** To ascertain whether transcription or translation is primarily controlled by *IRC3*, two conditional alleles of *IRC3* designated *irc3-1* and *irc3-2* were generated as described in Materials and Methods and further characterized. The altered amino acids are described in Table S3. Conditional alleles allowed us to examine the consequences on mitochondrial transcripts and newly synthesized protein products upon rapid depletion of active pools of Irc3 protein (see below).

Cells expressing either temperature-sensitive alleles or the wild-type allele of *IRC3* when cultured in glucose at the permissive temperature of 23°C gave rise to progeny that was able to utilize glycerol at the same rate. On the other hand, cells expressing either *irc3-1* or *irc3-2* when subcultured in glucose at the nonpermissive temperature of 37°C gave rise to

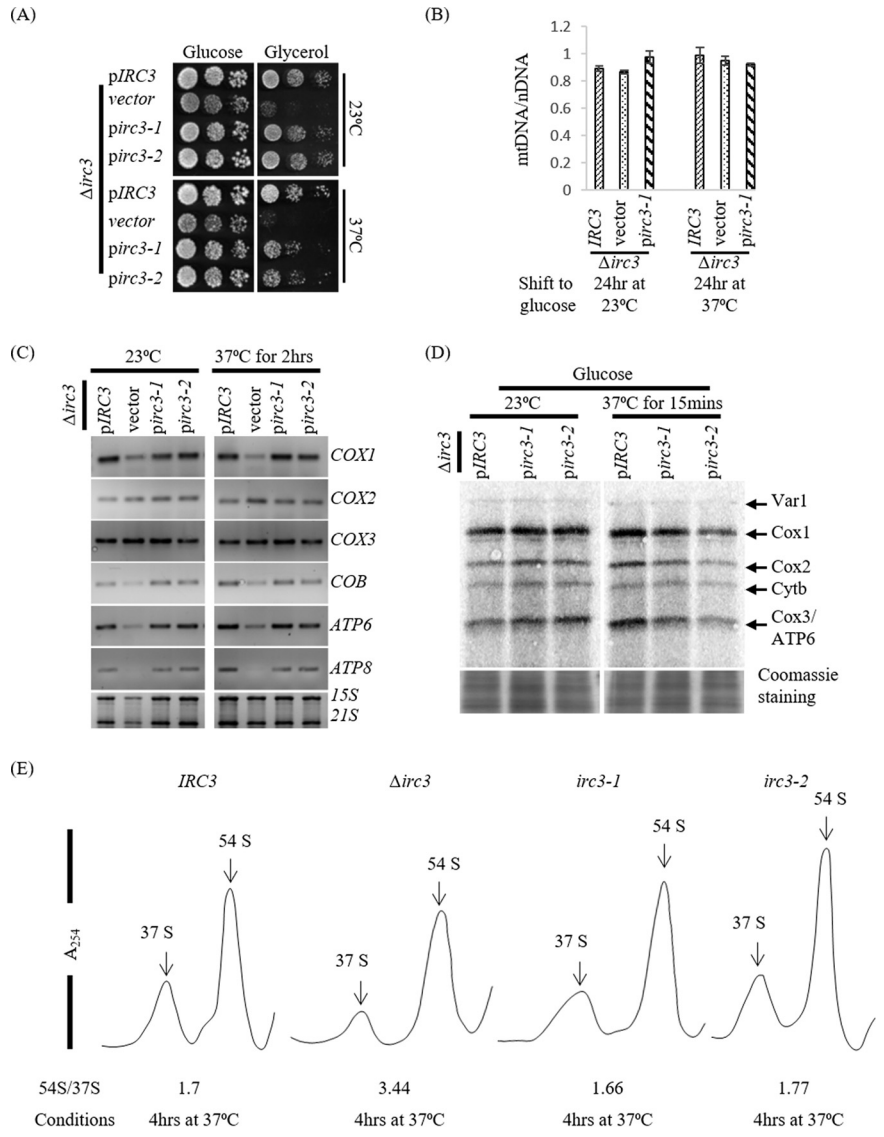

FIG 2 Rapid depletion of functional *IRC3* in cells grown in glucose leads to aberrant mitochondrial translation. (A) Tenfold serial dilutions of glucose-grown Δ*irc3*ρ^+ cells expressing either an episomal copy of *IRC3*, vector, *irc3-1*, or *irc3-2*, spotted on glucose and glycerol plates, and incubated at 23°C and 37°C are shown. (B) The ratio of nuclear to mitochondrial DNA was estimated in the indicated strains after subculturing in glucose for the indicated time period at 23°C or 37°C. (C) Transcript levels of mitochondrial genes were assayed in the indicated strains grown in glucose. 21S rRNA and 15S rRNA levels were detected by EtBr. Samples were normalized for total RNA. (D) Mitochondrial protein synthesis was measured in the indicated strains grown in glucose at either 23°C or after shift to 37°C for 15 min. Labeling reaction was carried out by incorporation of ^{35}S-labeled methionine and cysteine in the presence of cycloheximide to inhibit cytosolic protein synthesis at 23°C or 37°C for 30 min. Mitochondria from labeled cells were isolated, and equivalent mitochondrial proteins were separated on a 17.5% SDS-PAGE gel. Radiolabeled proteins were visualized by phosphorimaging. At the bottom is a Coomassie blue-stained gel of radiolabeled mitochondrial protein extracts. (E) Mitochondrial ribosomal subunits from the indicated strains cultured in glucose at 37°C for 4 h were separated on a 10-to-30% sucrose gradient. RNA content was monitored by measuring the absorbance at 254 nm. The positions of the 37S and 54S peaks are labeled. The relative ratio of the 54S/37S peaks is listed below each profile.

fewer progeny that could utilize glycerol (Fig. 2A). We confirmed that cells expressing either *irc3-1* or *irc3-2* retained mtDNA copy numbers similar to wild-type levels upon subculturing in glucose for 24 h at both at 23°C and 37°C (Fig. 2B; Fig. S2A).

To determine whether *IRC3* primarily regulates transcription, we measured the levels of mature transcripts by using reverse transcriptase PCR in cells harboring either *IRC3*,

irc3-1, or *irc3-2* cultured at either 23°C or after a shift to 37°C for 2 h. We found that levels of mitochondrial mRNA in *irc3-1* and *irc3-2* cells were similar to those in wild-type cells at 23°C or after shift to 37°C for 2 h (Fig. 2C). These results indicate that reduced steady-state levels of mitochondrial mRNA in the Δ*irc3*ρ^+ strain in glucose-grown cells (Fig. 2C and 1D) could be an indirect consequence of the loss of active pools of Irc3.

To determine whether Irc3p regulates mitochondrial translation, incorporation of ^{35}S-labeled methionine and cysteine into newly synthesized mitochondrial proteins was analyzed in *IRC3*, *irc3-1*, and *irc3-2* cells grown in glucose, galactose, and glycerol. Cells expressing *IRC3*, *irc3-1*, and *irc3-2*, when grown on glucose at 23°C, showed similar rates of incorporation of radiolabel into newly synthesized mitochondrial proteins (Fig. 2D). However, when cells were shifted to 37°C for 15 min, cells expressing temperature-sensitive alleles *irc3-1* and *irc3-2* showed reduced incorporation of ^{35}S-labeled methionine and cysteine in comparison to that of wild-type cells, indicating the involvement of Irc3 in optimal regulation of mitochondrial translation (Fig. 2D and Fig. S2B). Interestingly, incorporation of radiolabel in newly synthesized proteins was compromised to a greater extent in *irc3-2* cells than in *irc3-1* cells, which could be due to mutation at a different site (Table S3). These results indicate that synthesis of all mitochondrially encoded proteins is affected early upon depletion of the active pools of Irc3 in cells under growth conditions containing glucose as the carbon source.

To rule out the possibility that the protein translation defects observed in *irc3-1* or *irc3-2* mutant cells at 37°C were due to an indirect consequence of aberrant mitochondrial ribosomal assembly/stability, the mitochondrial ribosomes isolated from glucose-grown cultures of *IRC3*, Δ*irc3*ρ^+, *irc3-1*, and *irc3-2* cells after shift to 37°C for 4 h were separated on a sucrose density gradient. The relative ratios of large mitochondrial subunits (54S) to small mitochondrial ribosomal subunits (37S) and their levels were quantified and compared. The levels of mitochondrial small ribosomal subunits (37S) in Δ*irc3*ρ^+ cells were severely reduced, leading to altered 54S/37S ratios, whereas in wild-type, *irc3-1*, and *irc3-2* cells, similar 54S/37S subunit ratios and levels were observed upon a shift to 37°C for 4 h (Fig. 2E). This indicated that altered ratios in Δ*irc3*ρ^+ cells are an indirect consequence of disrupted mitochondrial function due to the absence of Irc3 rather than from a direct role for Irc3 to promote ribosome assembly. Since 54S/37S ratios are unchanged in *irc3-1*, *irc3-2*, and *IRC3* cells at 37°C, this indicates that the defective mitochondrial protein synthesis observed in *irc3-1* and *irc3-2* cells at 37°C is not an indirect consequence of defective mitochondrial ribosomal assembly/stability.

We have further observed that mitochondrial translation is regulated by *IRC3* differentially depending upon the available carbon source. Equivalent levels of newly synthesized mitochondrial proteins were observed in *IRC3*, *irc3-1*, and *irc3-2* cells that had been cultured in glycerol or galactose at 23°C or followed by incubation at 37°C for 2 h (Fig. S2C and S2D). Consistently, cells expressing *IRC3*, *irc3-1*, and *irc3-2* when cultured in glycerol and galactose at 23°C or 37°C gave rise to progeny that were able to utilize glycerol to the same extent (Fig. S2E and S2F). Reduction in levels of *de novo* Cox1p in Δ*irc3*ρ^+ cells (Fig. 1F) is unlikely to be due to defects in ribosome assembly/levels, as the 54S/37S ratios were similar in Δ*irc3*ρ^+ and *IRC3* cells cultured in glycerol for 12 h at 30°C (Fig. S4). Hence, taken together, our data support a role for Irc3 in regulating mitochondrial translation in response to metabolic cues.

Irc3p fractionates with small mitochondrial ribosomal subunits independent of metabolic cues. Given that IRC3 is a predicted RNA helicase and a reduction in functional *IRC3* in cells leads to aberrant mitochondrial protein synthesis suggest a role for Irc3p in mitochondrial translation initiation and elongation, either of which would require Irc3p to be associated with the mitochondrial ribosome. In the absence of antibodies to the endogenous protein, to detect Irc3 within the mitochondria, we tagged *IRC3* with 13×myc at the C terminus. We confirmed that *IRC3-myc* encodes a functional protein localized to the mitochondria (Fig. S3A and S3B). Interestingly, we had observed that mitochondrial translation was perturbed to different levels in cells expressing *IRC3* mutants when cultured under conditions that maintain mitochondrial OXPHOS function at basal or elevated levels (Fig. 1F and 2D; Fig. S2B and S2C). Thus, we determined whether Irc3-myc physically associates with mitochondrial ribosomes in exponentially growing cells cultured in glucose and glycerol. In addition, we examined the association of Irc3-myc with mitochondrial ribosomes in cells that had attained stationary phase. Mitochondrial ribosomes were separated on a 10-to-30% sucrose gradient as described

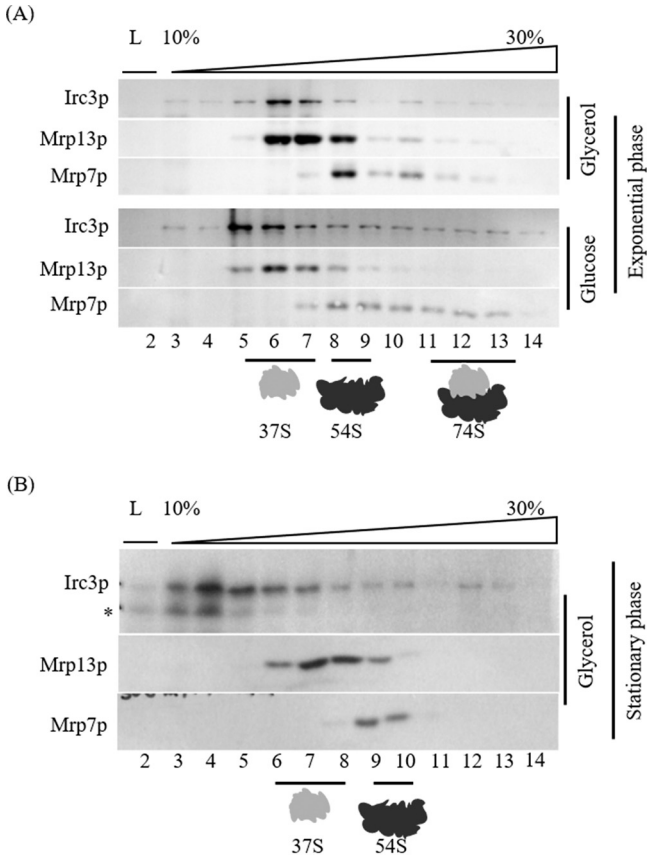

FIG 3 Irc3p associates with small subunits of mitochondrial ribosome during exponential growth phase. Mitochondrial ribosomes from cells expressing functional *IRC3-Myc*, which are cultured either in glucose or glycerol to exponential phase (A) or in glycerol to stationary phase (B) were separated by ultracentrifugation on a 10-to-30% sucrose gradient containing 400 mM NH_4Cl at 135,000 $\times$ *g* for 4 h. Equivalent protein fractions were TCA precipitated, separated on an SDS-PAGE gel, and subjected to immunoblot analysis using antibodies against c-Myc, Mrp7p, and Mrp13p. The positions of 37S, 54S, and 74S are shown at the bottom. The uppermost fraction of sucrose gradient upon centrifugation is labeled as L. An asterisk indicates a cross-reacting signal obtained from anti-Myc antibody likely to be a cleavage product of Irc3 during sample processing.

in Materials and Methods, and individual fractions were probed for the presence of Mrp7 and Mrp13 to ascertain the fractions containing the 37S small subunit and 54S large subunit. Irc3-myc peaked in fractions containing Mrp13 in mitochondria from exponentially growing cells cultured in glycerol and glucose (Fig. 3A). A small proportion of the total signal from Irc3-myc also cofractionated with both Mrp7 and Mrp13, indicating an association with a 74S subunit in mitochondria from exponentially growing cells cultured in glucose and glycerol (Fig. 3A). In contrast, when mitochondrial ribosomes were separated on a sucrose gradient from stationary-phase cells cultured in glycerol, the majority of Irc3-myc was found at the top of the gradient and only a small fraction of the Irc3-myc pool was present in fractions containing Mrp7, followed by a minor pool in heavier fractions (Fig. 3B).

Irc3p is involved in mitochondrial translation elongation. The absence of or reduction in active pools of Irc3 led to reduced mitochondrial protein synthesis. This could be due to a defect in either translation initiation or elongation or both. To directly examine the role of *IRC3* in translation initiation from mitochondrial mRNA, we used engineered strains YC162, RG140, and RG139, carrying a mitochondrial reporter gene in Δ*irc3* cells expressing either *IRC3*, vector, *irc3-1*, or *irc3-2*. In these strains, arginine 8 (Arg8), an essential matrix-localized enzyme required for arginine biosynthesis, has been deleted from the nuclear genome and a recoded version termed $Arg8^m$ is expressed from the mitochondrial DNA, specifically replacing the coding sequences of Cox1, Cox2, and Cox3 and keeping the 5′ and 3′ UTRs intact (Fig. S5) (62). Functional mitochondrial translation initiation in these strains can be scored based on the

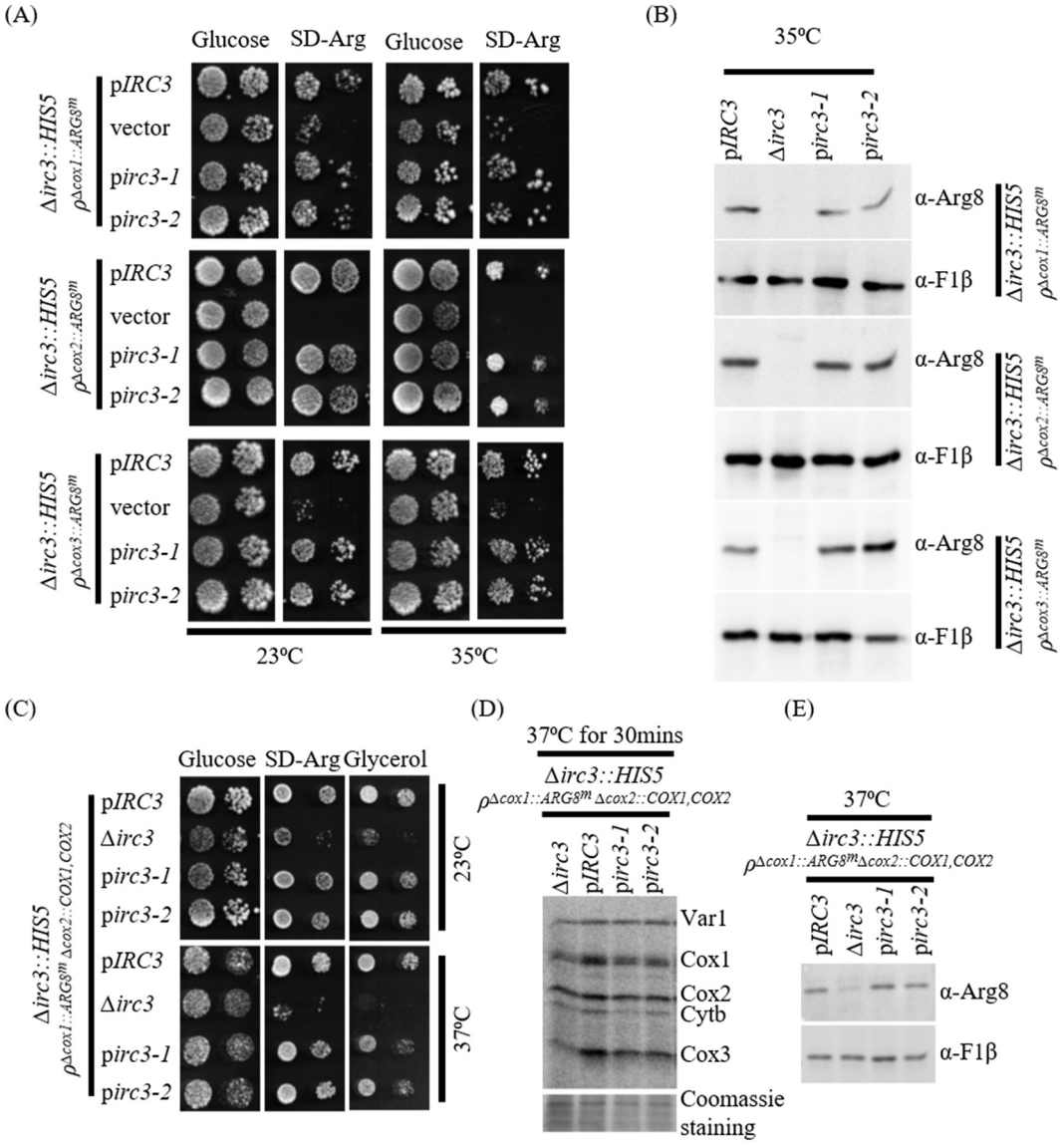

FIG 4 Irc3p regulates mitochondrial translation elongation and not initiation. (A) Serial dilutions of Δ*irc3*ρ^+cells expressing either a wild copy of *IRC3*, vector, *irc3-1*, or *irc3-2* harboring mtDNA modified to carry Arg8^m reporter cassettes in place of *COX1*, *COX2*, and *COX3* open reading frames were cultured in glucose prior to spotting on glucose and synthetic medium lacking arginine and incubated at the indicated temperature. (B) Steady-state levels of mitochondrial Arg8^m were measured by immunoblot analysis in the indicated strains at the nonpermissive temperature. Anti-F1β was used as a loading control. (C) Serial dilution of Δ*irc3*ρ^+ cells expressing either a wild-type copy of *IRC3*, vector, *irc3-1*, or *irc3-2* harboring mtDNA expresses Arg8^m reporter cassette in place of *COX1* ORF, while *COX1* and *COX2* ORF were placed under *COX2* 5′ and 3′ UTRs cultured in glucose prior to spotting on glucose, glycerol, and synthetic media lacking arginine and incubated at indicated temperatures. (D) Mitochondrial protein synthesis was measured in the indicated strains upon shift from 23°C to 37°C for 30 min. Labeling reaction was carried out by incorporation of ^{35}S-labeled methionine and cysteine in the presence of cycloheximide to inhibit cytosolic protein synthesis at 37°C for 30 min. Mitochondria from labeled cells were isolated, and equivalent amounts of proteins were separated on a 17.5% SDS-PAGE gel. Radiolabeled proteins were visualized by phosphorimaging. At the bottom is a Coomassie blue-stained gel of radiolabeled mitochondrial protein extracts. (E) Steady-state levels of mitochondrial Arg8^m and F1β were measured in the indicated strains cultured at 37°C.

ability of cells to grow on synthetic plates lacking arginine (SD-Arg; where SD is 0.67% yeast nitrogen base without amino acids containing 2% glucose). YC162, RG140, and RG139 deleted for *IRC3* showed a growth defect on SD-Arg with reduced Arg8^m protein accumulation in mitochondria (Fig. 4A and B), consistent with multiple defects in mitochondrial gene expression (Fig. 1). However, engineered Δ*irc3* cells episomally expressing either the *irc3-1* and *irc3-2* allele showed growth rates similar to that of wild-type cells on SD-Arg at both permissive and nonpermissive temperatures (Fig. 4A). Consistently, steady-state levels of Arg8^m in mitochondria

from cells cultured at a nonpermissive temperature were also similar in these cells (Fig. 4B). These results indicate that although *IRC3* is a key regulator of mitochondrial translation, defects observed after rapid depletion of active pools of Irc3 do not severely compromise the initiation process.

To differentiate the role of *IRC3* more specifically in mitochondrial translation initiation and elongation, we used engineered strains XPM171a and XPM78a with a mitochondrial reporter gene in Δ*irc3*ρ^+ cells expressing either *IRC3*, vector, *irc3-1*, or *irc3-2*. In XPM171a, the recoded Arg8^m gene was placed under the control of *COX1* 5′ and 3′ UTRs, while *COX1* and *COX2* open reading frames (ORFs) were placed under the control of *COX2* 5′ and 3′ UTRs (Fig. S5) (27). This allows translation initiation to be monitored as a function of growth on SD-Arg and translation elongation to be scored as a function of growth on glycerol (YPG [1% yeast extract, 2% peptone, 3% glycerol]). When cells were cultured in glucose medium, Δ*irc3* cells were severely defective for growth on SD-Arg and YPG in comparison to wild-type cells (Fig. 4C), consistent with compromised mitochondrial gene expression (Fig. 1). In contrast, Δ*irc3* cells episomally expressing either the *irc3-1* or *irc3-2* allele were defective for growth on YPG but not SD-Arg at 37°C in comparison to *IRC3* cells, while at 23°C, *IRC3*, *irc3-1*, and *irc3-2* cells grew at similar rates on both SD-Arg and YPG (Fig. 4C). Consistent with a defect in translation elongation in glucose-cultured cells, we found that incorporation of ^{35}S-labeled methionine and cysteine into newly synthesized Cox1 as well as other mitochondrial encoded proteins were reduced in Δ*irc3*ρ^+, *irc3-1*, and *irc3-2* cells upon shift to 37°C from 23°C for 30 min (Fig. 4D). Consistent with no significant defects in translation initiation, Δ*irc3*ρ^+ cells episomally expressing either *IRC3*, *irc3-1*, or *irc3-2* at 37°C accumulated similar levels of Arg8^m in the mitochondria (Fig. 4E).

XPM78a expresses 512 nucleotides of intronless *COX1* fused to Arg8^m under the control of *COX1* 5′ and 3′ UTRs (Fig. S5A). Within the Arg8^m sequence, the cleavage site for pre-Arg8 is present, such that Cox1 and Arg8^m function independently (27). This allows translation elongation to be scored on SD-Arg and glycerol plates. Cells harboring the Δ*irc3* allele were compromised for growth on both SD-Arg and glycerol in comparison to the wild type (Fig. S5B). Consistently, incorporation of ^{35}S-labeled methionine and cysteine into newly synthesized Cox1 and Arg8^m and steady-state Arg8 levels in Δ*irc3* cells were reduced in comparison to that of wild-type cells (Fig. S5C and S5D). Growth defects in Δ*irc3*ρ^+cells expressing *irc3-1* and *irc3-2* on SD-Arg and glycerol plates could not be ascertained, as there was a drastic loss of cell viability at the nonpermissive temperature when the cells were incubated for more than 6 h (data not shown). In addition, we were not able to visualize the Cox1-Arg8 fusion product, likely due to its labile nature. Taken together, these results indicate that Irc3p is involved in mitochondrial translation elongation.

Rho suppressors of the Δ*irc3* strain restores translation differentially based on metabolic cues. We have shown that Irc3p regulates mitochondrial translation differently in cells based upon the carbon source available for growth. Identification of suppressors of deletion strains often leads to revelation of novel genetic networks in play. Thus, we isolated spontaneous Δ*irc3*ρ^+ suppressors by using two independent strategies. In the first screen, Δ*irc3*ρ^+ suppressors were identified by plating the Δ*irc3*ρ^+ strain for single-cell colonies on solid medium containing glycerol. Cells that were able to utilize glycerol at a higher rate were initially scored as suppressors. Two Δ*irc3* suppressors (Δ*irc3*ρ^{SUP1} and Δ*irc3*ρ^{SUP2}) that were able to maintain growth in respiratory medium after repeated subculturing in glucose were analyzed further (Fig. 5A). A second independent screen used the Δ*irc3*ρ^+ strain carrying an unlinked *ade2* mutation in the background. Strains carrying an *ade2* mutation are red in color when grown in glucose as long as their mitochondrial function is intact, as are strains carrying *IRC3* and *ade2* (Fig. 5A). Strains with compromised mitochondrial function that are deficient for respiration are white in color (63, 64), as are, e.g., Δ*irc3*,*ade2* strains (Fig. 5A). To find second-site Δ*irc3* suppressors, Δ*irc3*, *ade2* cells were plated on solid glucose medium and scored for red colony sectors. Four suppressors (Δ*irc3*,*SUP3*ρ^+, Δ*irc3*ρ^{SUP4}, Δ*irc3*ρ^{SUP5}, and Δ*irc3*ρ^{SUP6}) were identified and further confirmed for growth on glycerol medium (Fig. 5A). Interestingly, the suppressors identified by the first screen formed white colonies on glucose plates in spite of the presence of an *ade2* mutation, and on glycerol plates, the colony size was larger than that of the wild type (Fig. 5A).

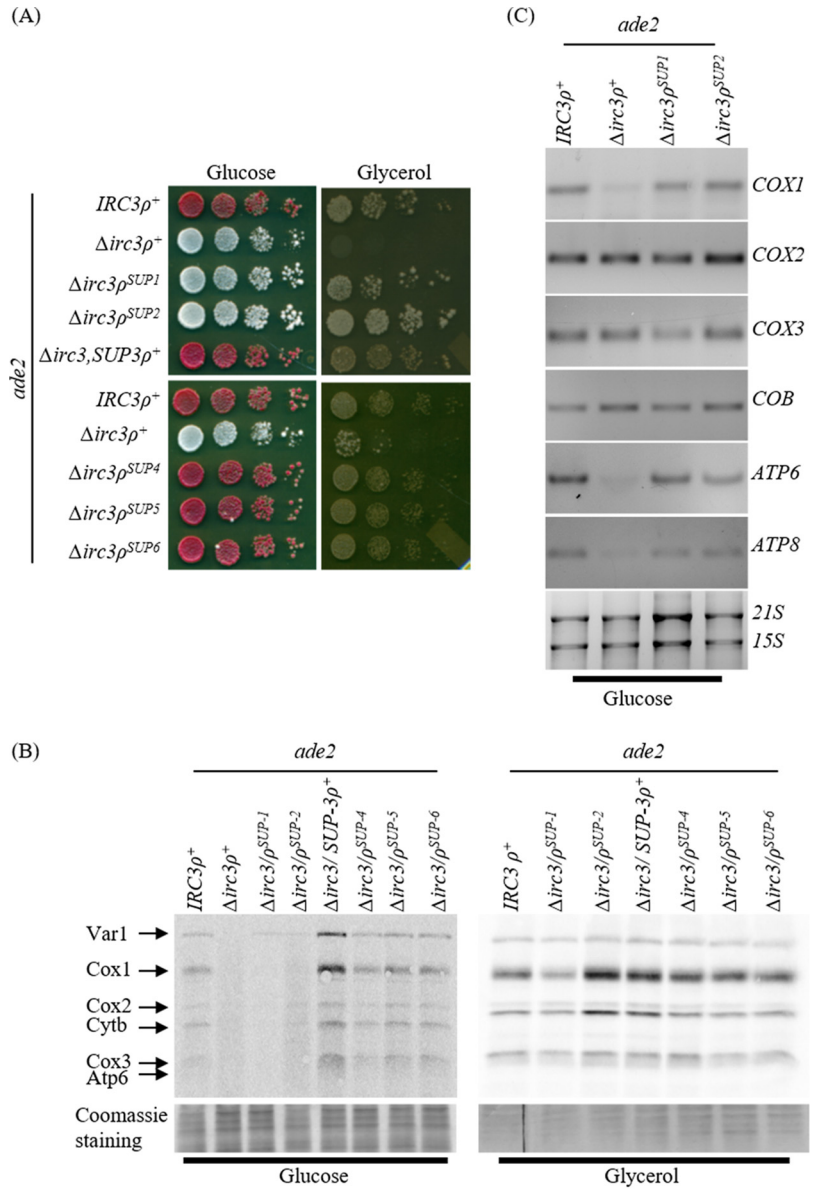

FIG 5 Restoration of mitochondrial protein synthesis in Δ*irc3*ρ^+ suppressors is dependent on the carbon source used for cell growth. (A) Tenfold serial dilutions of the wild type and Δ*irc3*$\rho^+$and Δ*irc3*ρ^+ suppressors spotted on glucose and glycerol plates are shown. (B) Mitochondrial protein synthesis was measured in wild-type, Δ*irc3*ρ^+, and the indicated Δ*irc3*ρ^+ suppressor strains cultured in glucose and glycerol at 30°C. Labeling reaction was carried out by incorporation of ^{35}S-labeled methionine and cysteine in the presence of cycloheximide to inhibit cytosolic protein synthesis at 30°C for 30 min. Mitochondria from labeled cells were isolated, and proteins were separated on a 17.5% SDS-PAGE gel. Radiolabeled proteins were visualized by autoradiography. At the bottom is a Coomassie blue-stained gel of radiolabeled mitochondrial extracts. (C) Transcript levels of the indicated mitochondrial genes were assayed in wild-type, Δ*irc3*ρ^+, Δ*irc3*ρ^{SUP1}, and Δ*irc3*ρ^{SUP2} cells under glucose culture conditions. 21S rRNA and 15S rRNA levels were detected by EtBr staining.

Diploids generated by crossing the suppressor strains with the Δ*irc3*ρ^0 strain retained the ability to grow on glycerol, thereby indicating that the suppressor mutation was dominant in character. Among the six suppressors identified, five suppressors contained a mutation in the mitochondrial genome and one suppressor contained a mutation in the nuclear genome, as determined based on the crosses described (Fig. S6). As we have shown before that Irc3 regulates mitochondrial translation differentially in glucose-grown cultures and galactose/glycerol-grown cultures, we determined whether mitochondrial translation was restored to the same levels in all suppressors

cultured in glucose or glycerol. We found that incorporation of ^{35}S-labeled methionine and cysteine into newly synthesized mitochondrial proteins were restored to wild-type levels in Δ*irc3,SUP3*ρ^+, Δ*irc3*ρ^{SUP4}, Δ*irc3*ρ^{SUP5}, and Δ*irc3*ρ^{SUP6} strains independent of carbon source in the growth medium (Fig. 5B). Interestingly, in Δ*irc3*$\rho^{SUP1}$and Δ*irc3*ρ^{SUP2} strains, mitochondrial translation was restored to nearly wild-type levels when glycerol was used as a carbon source in growth medium. However, mitochondrial translation was not restored to wild-type levels when glucose was used as a carbon source in growth medium (Fig. 5B). Levels of mitochondrial mRNA were similar in Δ*irc3*ρ^{SUP1} and Δ*irc3*ρ^{SUP2} suppressors and in wild-type cells grown in glucose, indicating that reduced translation levels in glucose-grown cells were not due to reduced transcript levels of mitochondrial mRNA (Fig. 5C). These results further indicate that Irc3 regulates mitochondrial translation and that the mode of regulation is dependent on the carbon sources available for cell growth.

DISCUSSION

Translation is a multistep process involving initiation and peptide elongation followed by termination and ribosome recycling. Translation rates are regulated by numerous protein factors and mRNA secondary structures that vary with environmental conditions (65). In mitochondria, the translation system has an added layer of complexity, where the machinery is tightly associated by the mitochondrial inner membrane and requires membrane-embedded mRNA-specific translation activator for protein synthesis (4). These presumably are the reasons why a membrane-free *in vitro* translation system has not yet been developed, and the mechanism underlying mitochondrial protein synthesis remains poorly understood.

In this study, we used genetic and biochemical methods to investigate the role of the putative DExH/D helicase gene *IRC3*, which could be speculated to modify structures involving either DNA-DNA or RNA-RNA or DNA-RNA hybrids during mitochondrial DNA synthesis/repair and gene expression, respectively. We observed that cells deleted for *IRC3* rapidly lose the ability to utilize glycerol as the sole carbon source, followed by a relatively low rate of mitochondrial DNA loss (Fig. 1), consistent with previously reported examples of proteins required for mitochondrial gene expression (43, 49, 50). Furthermore, we demonstrate as expected for a protein to regulate mitochondrial translation, Irc3-myc cofractionates with mitochondrial small ribosomal subunits (Fig. 3A), deletion of *IRC3* led to decreased mitochondrial translation (Fig. 1), and Δ*irc3*ρ^+ suppressors restored mitochondrial translation to distinct levels in response to metabolic cues (Fig. 5). Although the precise molecular details by which Irc3 regulates mitochondrial translation is unknown, our results support a model where Irc3 regulates translation elongation. First, upon direct examination of mitochondrial translation in *irc3-1* and *irc3-2* cells, we observed a decrease in *de novo* polypeptide synthesis upon shift to the nonpermissive conditions within the first 15 min (Fig. 2). Second, using the Arg8^m reporter gene, we observed that Irc3 is required specifically for translation elongation (Fig. 4; see Fig. S5 in the supplemental material).

It has been well established that in response to metabolic cues (glucose versus galactose/glycerol), yeast cells differentially regulate gene expression (66–70). Culturing cells in glucose, galactose, or glycerol leads to differential utilization of mitochondrial OXPHOS for ATP production. In glucose, mitochondrial OXPHOS activity is maintained at basal levels, while in galactose or glycerol, this activity is elevated (71, 72). A shift of yeast cells from glucose to galactose/glycerol leads to increased translation of nuclear and mitochondrially encoded OXPHOS subunits. Increased mitochondrial translation is brought about as a consequence of upregulated expression of nucleus-encoded mRNA-specific translation activators (22, 23, 73). Could additional molecular factors with novel mechanisms that modulate mitochondrial translation in response to carbon source exist? We found that Irc3 differentially regulates mitochondrial translation when cells are cultured under conditions which require OXPHOS at basal versus elevated levels (Fig. 1 and 2; Fig. S2). When glucose is used as the carbon source, protein translation in Δ*irc3*ρ^+ mitochondria is defective for all transcripts, whereas when galactose is used as the carbon source, protein translation from Cox1 mRNA is predominantly reduced. This contrasts with the observation that accumulation of mitochondrial transcripts was disrupted to the same extent

irrespective of carbon source used for growth (Fig. 1). When *irc3-1* and *irc3-2* cells were cultured in glucose at restrictive temperatures, the rates of protein translation mirrored protein translation rates from Δ*irc3*ρ^+ cells albeit to a less severe level. This could be due to expression of partially functional proteins from *irc3-1* and *irc3-2* alleles that are distinctly labile at elevated temperatures. However, when *irc3-1* and *irc3-2* cells were cultured in galactose or glycerol at restrictive temperatures, mitochondrial translation was not altered, and their progeny cells were not defective for growth on glycerol. Coincidentally, our screening for temperature-sensitive mutants was biased toward disrupting *IRC3* function specifically in glucose-cultured cells. Thus, taken together, these findings lead one to speculate that Irc3p differentially regulates mitochondrial translation in response to metabolic cues.

Genetic suppressors have been routinely used to understand cellular networks that play intertwined roles. We screened for Δ*irc3*ρ^+suppressors, based on the ability to restore normal mitochondrial function in either glucose or glycerol. Intriguingly, Δ*irc3*ρ^+ suppressors that were isolated restored mitochondrial translation to different extents based on the carbon source added to the growth medium. Δ*irc3*ρ^+ suppressors that were isolated for restoration of mitochondrial function on glycerol restored mitochondrial translation to wild-type levels only when glycerol and not glucose was the carbon source added to the growth medium. In contrast, Δ*irc3*ρ^+suppressors that were isolated for restoration of mitochondrial function on glucose restored mitochondrial translation to the same extent irrespective of whether glucose or glycerol was provided for cell growth (Fig. 5). Although it is not possible to comment on the exact nature of the suppressor mutation(s), it leads to increased processivity of the translation machinery. A mutation(s) on mtDNA in glucose-derived suppressors likely increases the translation processivity to a greater extent than that in glycerol-derived suppressors. Could this difference in translation processivity in Δ*irc3*ρ^+suppressors hypothetically indicate the existence of altered mRNA structures of various degrees of compactness in mitochondrial transcripts between cells grown in glucose versus glycerol? It is not completely understood how mRNAs fold into compact structures in the cell. However, secondary and tertiary structures in the 5′ UTR, coding sequence (CDS), and 3′ UTR are well described regulators of essential processes such as translation initiation, translation elongation, ribosomal traffic jams, and mRNA stability (reviewed extensively in references 74 to 77). Ribosome processivity during the process of translation elongation is believed to be the principal mechanism that leads to its secondary-structure resolution within the CDS (78–80). Interestingly, in glucose-grown yeast cells, mitochondrial transcripts are abundant, although their translation is at the basal level. Upon a shift to glycerol, increases in individual mRNA translation rates are greater than increases in their transcription rates (22, 81). Thus, one could imagine that compact mRNA molecules contribute to the previously described basal translation rates in glucose. Conversely, when glycerol is the carbon source for cell growth, less-compact mitochondrial mRNA structures exist, possibly because of the enhanced level of association with the ribosomes, requiring Irc3 for translation of a subset of mRNA such as for Cox1.

How could Irc3p differentially regulate mitochondrial translation when associated with mitochondrial small ribosomal subunits in both glucose and glycerol? Two nonexclusive hypothetical models could be invoked to address this question, both of which require Irc3's association with different interacting partners. These interacting partners could be proteins whose expression is controlled by metabolic cues, such as those that have been described as a part of large-scale proteome remodeling that occurs when cells are shifted from glucose to galactose/glycerol (22). In the first model, these protein partners in association with Irc3 target the regions of mRNA with compact local secondary RNA structures that are maintained in the mitochondria as a function of their growth condition and which require unwinding during translation elongation. An alternate model could be that these distinct interacting partners for Irc3 are associated with the compact mRNA structures. During the process of translation elongation, Irc3 bound to the small subunit is responsible for displacing these proteins, thereby melting or unwinding the structures required for translation elongation. Future

experiments targeted to parsing the mechanism by which Irc3 regulates mitochondrial translation will require these hypothetical models to be accounted for.

Deletion of *IRC3* has previously been reported to accumulate double-stranded mitochondrial DNA breaks (47). ATPase activity of the Irc3 protein is essential *in vivo* and is stimulated *in vitro* by DNA molecules, especially those mimicking recombination intermediates (47, 48, 82). Here, we have clearly shown that *IRC3* is required for mitochondrial translation *in vivo*. It is not well understood why disruption of mitochondrial translation often leads to loss of mitochondrial DNA. Is it possible that SFII DExH helicases can target both mtDNA and mitochondrial mRNA, thereby forming a link between optimal translation and mtDNA stability? Among the four annotated SFII DExH helicases, SUV3, which is the RNA helicase component of the mitochondrial exoribonuclease complex in addition to having a role in RNA turnover (44, 46), has also been implicated in mitochondrial genome stability (83–85). A similar link between ribosome biogenesis with DNA replication has been found in both bacteria and yeast. In bacteria, Obg GTPases, which are known to control large ribosomal subunit biogenesis (86, 87), link essential processes required for cell cycle progression, such as DNA replication, by a yet unknown mechanism (88–91). Nog1, the nucleolar member of the Obg family of GTPases in yeast which is required for 60S ribosomal subunit biogenesis (92, 93), is also associated with the origin recognition complex in yeast (94, 95). Interestingly, we found Irc3 to predominantly cofractionate with mitochondrial ribosomes in cells that are in logarithmic growth phase. However, in cells that have entered stationary phase, only a small fraction of Irc3 is cofractionated with mitochondrial ribosomes (Fig. 3). It is interesting to speculate that Irc3 during rapid growth is involved in the regulation of mitochondrial translation and switches to mtDNA maintenance at other times, thus establishing a link between these two processes.

Mitochondrial functioning vis-à-vis ATP generation is altered depending on whether the cell is poised for rapid proliferation or in a quiescent/differentiated state. Proliferating cells, including pluripotent stem cells, use glycolysis even in the presence of oxygen, whereas differentiated cells use mitochondrial oxidative phosphorylation (96–98). *Saccharomyces cerevisiae* shows a similar plasticity in response to metabolic cues; i.e., when grown aerobically in glucose, yeast cells derive ATP from fermentation while producing ethanol as a by-product. Under these conditions, the metabolism in yeast cells is akin to proliferating mammalian cells. Upon exhaustion of glucose, yeast cells switch to oxidative phosphorylation for ATP generation from the ethanol produced during fermentation to sustain itself, akin to differentiated cells (99, 100). We have shown that *IRC3* regulates mitochondrial translation distinctively in yeast mitochondria in response to metabolic cues. The closest orthologue for IRC3 in humans based on BLAST is an uncharacterized putative RNA helicase (GenBank accession no. BAG50877) that shares 24% identity and 39% similarity within the helicase core only and is predicted to localize to mitochondria with 84% probability (101). Thus, although a clear orthologue for *IRC3* is not present in mammalian cells, one could speculate that a similar mechanism exists in mammalian mitochondria to control synthesis of the OXPHOS protein complex whereby energy demands and signals governing the cellular state are integrated.

MATERIALS AND METHODS

Yeast strain, primers, and media. The yeast strains used are listed in Table S1 in the supplemental material. The sequences of primers used are listed in Table S2. The complete media used were YEP (1% yeast extract and 2% peptone) containing 2% glucose (YPD), 2% galactose (YPGal), or 3% glycerol (YPG) as a carbon source. Synthetic minimal media (0.67% yeast nitrogen base without amino acids containing 2% glucose [SD], 2% galactose [SGal], 3% glycerol [SG], 0.1% 5-fluoro-orotic acid and 2% glucose (5FOAD), or 0.006% canavanine sulfate and 2% glucose [SCAN]) were supplemented with the appropriate amino acids when required, as described previously (102).

Generation of plasmids and strains. To generate an episomally expressed *IRC3*, *IRC3* with 634 bp upstream of the start codon and 1 kb downstream of the stop codon in addition to the ORF was PCR amplified using the *YDR332w*up and *YDR332w*dn primer pair (Table S2) and cloned into pRS426 and pRS315 at the NotI site to generate pRS426:*IRC3* (pJk20) and pRS315:*IRC3* (pJk22). In order to generate a construct expressing *IRC3* with C-terminally tagged Myc under its endogenous promoter pRS315::*IRC3-Myc*, Myc-KanMX6 was amplified from the pFA6a-13Myc-kanMX6 plasmid (103) by using the P3 and P4 primer pair (Table S2) and cloned into a pGEM-T easy vector at the TA cloning site to generate pJK55 (KDB784). *Myc-KanMX6* from pJK55 was subcloned into pJK34 (*IRC3*::3HA) as a BamHI and SalI fragment to generate pJK52 (KDB698).

Cells deleted for *IRC3* were generated in a diploid strain (KDY335) created by crossing CRY1 (*MATα ura3-52 trp1Δ2 leu2-3_112 his3-11 ade2-1 can1-100*) and BY4742 (*Matα his3Δ1 leu2Δ0 lys2Δ0 ura3Δ0*). Disruption of *IRC3* was carried out by using a PCR-based gene replacement approach, in which the *Schizosaccharomyces pombe HIS5* gene was amplified from pFAa-His3MX6 (103) with upstream and downstream regions of *IRC3* by using PCR using oligonucleotides F1 and R1 (Table S2). The linear PCR product was transformed into a diploid strain (KDY335) to create a heterozygous diploid strain (KDY394). A plasmid-borne *IRC3* (pJK20) was transformed into a heterozygous diploid strain (KDY394) and sporulated, and haploid spores were selected on SCAN to generate a strain with a chromosomal copy of *IRC3* deleted and Irc3 expressed episomally with intact mitochondrial DNA (KDY495). In order to eliminate the chance of creating a mutation at a second site in the genome during generation of Δ*irc3::HIS5* and to possess mtDNA from an isogenic strain, KDY495 was backcrossed six times with BY4741. The haploid strain generated upon backcrossing was named KDY1146. Replacement of the wild-type copy of *IRC3* with *HIS5* was similarly carried out in YC162, RG139, RG140, and W303ρI^0 to generate KDY1575, KDY1529, KDY1531, and KDY1589, respectively.

In order to study translation initiation and elongation, the Δ*irc3* strain carrying the ARG8^m reporter cassette was created by crossing KDY1146 ρ^0 with XPM171a and XPM78a, respectively. Diploid cells were sporulated, and haploid spores were selected on SCAN, lacking arginine and histidine. To ensure that the arginine gene from the nuclear genome in the haploids is disrupted, mitochondrial DNA was removed by growing cells in YPD supplemented with 25 μg/ml ethidium bromide (EtBr) and tested for growth on SD plates lacking arginine. The corresponding cells unable to grow on SD plates lacking arginine were selected from YPD plates, and the absence of the *IRC3* gene from the nuclear background was confirmed by PCR using YDR332wup and YDR332wdn/R1 primers (Table S2) to generate KDY1447 and KDY1540.

Presence of mitochondrial DNA. The presence of mitochondrial DNA in Δ*irc3* cells expressing either *IRC3* (KDY1355) or empty vector (KDY1366) was measured by crossing cells with *IRC3* ρ^0 testers, followed by selection of diploid cells. The percentage of diploid cells that were able to utilize both glycerol and glucose was indicative of the presence of mtDNA in the haploid strain.

To measure the mitochondrial DNA copy number with respect to nuclear DNA in Δ*irc3* cells expressing either *IRC3* (KDY1355) or empty vector (KDY1366), total yeast DNA was isolated and quantitative PCR (qPCR) was performed using primers COX2L and COX2R for Cox2 amplification and ActinF.P and ActinR.P for actin amplification (Table S2). The ratio of signal for Cox2 to actin was used as a measure of the ratio of mitochondrial DNA to nuclear DNA, respectively.

Generation of temperature-sensitive (ts) allele of *IRC3*. Temperature-sensitive *irc3* alleles were created using error-prone PCR as described previously (104). The coding region was amplified by using the tsmutantF.P and *YDR332w*dn primer pair (Table S2). PCRs were carried out in the presence of a 5:1 ratio of (dTTP + dCTP):(dATP + dGTP) or (dATP + dGTP):(dTTP + dCTP). The concentration of $MnCl_2$ was varied from 0.3 to 0.5 mM. The resulting mutated PCR fragment was cloned by gap repair into pJK22. Linearized pJK22 (digested with NsiI) and mutagenized PCR product were cotransformed into KDY494. Transformed cells were selected on SD plates lacking leucine and uracil and patched on 5FOAD to negatively select for *URA3* helper plasmid expressing the wild-type allele of *IRC3*. Cells were then patched on glucose plates and incubated at 23°C and 37°C for 2 days. Cells were patched onto glycerol plates and scored for colony formation at the permissive temperature (23°C) but not at the nonpermissive temperature (37°C). Plasmid DNA was isolated from Δ*irc3* cells harboring putative temperature-sensitive alleles and amplified in *Escherichia coli* and sequenced. Two confirmed temperature-sensitive alleles of *IRC3* (pJK90 [KDB1019] and pJK93 [KDB1061]) were shuttled into KDY1146 and confirmed for growth at 23°C and not 37°C on YPG.

Isolation of mitochondria and separation of mitochondrial ribosomes. Mitochondria were isolated from cells grown in YPGal, YPD, or YPG at the indicated temperature at an optical density at 600 nm (OD_{600}) of 1 or 3. Mitochondria were isolated by a previously described method (105) with slight modifications as described previously (49). Mitochondrial ribosomes were separated by a sucrose density gradient as described previously (106). Mitochondria were resuspended in buffer D (10 mM Tris-Cl, pH 7.4, 10 mM magnesium acetate, 100 mM NH_4Cl, 7 mM β-mercaptoethanol, and 1 mM phenylmethylsulfonyl fluoride [PMSF]) and incubated on ice for 2 h to generate mitoplasts. Mitoplasts were harvested by centrifugation at 12,000 $\times$ *g* for 10 min, resuspended in buffer D containing 2% NP-40, and further incubated on ice for 30 min to allow swelling. Mitochondrial lysis was achieved by 20 strokes with a tight-fitting pestle Dounce homogenizer. The mitochondrial lysate was clarified by centrifugation at 40,000 $\times$ *g* for 25 min. An equivalent number of clarified lysates was loaded onto a 10-to-30% sucrose gradient containing 10 mM Tris-Cl, pH 7.4, 10 mM magnesium acetate, 7 mM β-mercaptoethanol, and 400 mM NH_4Cl. Ribosomal particles were centrifuged at 135,000 $\times$ *g* for 4 h in a Beckman SW41Ti rotor. Equivalent fractions were collected, and RNA contents were measured by UV absorbance at 254 nm using an ISCO continuous-flow cuvette. Protein samples in each fraction were precipitated using 15% trichloroacetic acid (TCA), separated by SDS-PAGE, and subjected to immunoblot analysis.

Analysis of mitochondrial transcripts. Cells were grown in either YPD or YPGal medium or shifted to YPG medium. Cells were collected by centrifugation at 2,660 $\times$ *g* for 5 min, washed with water, and resuspended in SB3 buffer (50 mM Tris-Cl, pH 8, 10 mM $MgCl_2$, 3 mM dithiothreitol [DTT], 1 M sorbitol). Spheroplasts were generated by treatment with Zymolyase (2.5 mg/g cell pellet) for 2 h at 37°C. Spheroplasts were collected by centrifugation at 4,000 $\times$ *g* for 5 min and further lysed by 20 strokes of a Dounce homogenizer. Cell lysate was centrifuged at 1,500 $\times$ *g* for 5 min at 4°C to remove cell debris. Supernatant was collected and centrifuged at 17,550 $\times$ *g* for 15 min at 4°C to pellet the mitochondria. Mitochondria were lysed by the addition of TRIzol, followed by chloroform. The aqueous layer containing mitochondrial nucleic acid was separated and precipitated by the addition of 3 M sodium acetate and isopropanol. The pellet was washed twice with 70% ethanol to remove excess salts and resuspended in water. Isolated RNA was further purified by adding 1 volume

of 2 M potassium acetate, pH 4.8, incubated on ice for 30 min, and centrifuged at 13,000 rpm and 4°C for 20 min. Precipitated RNA was treated with DNase I (2,000 U/ml) for 30 min at 37°C to remove contamination of nuclear or mtDNA, followed by precipitation with 3 M sodium acetate and isopropanol. Precipitated RNA was washed twice with 70% ethanol and resuspended in water. cDNA using random primers was synthesized from 25 ng/μl of RNA template. Synthesized cDNA was diluted 5 times prior to utilization in semiquantitative PCRs with a 23-cycle extension for mitochondrial genes *COX1*, *COX2*, *COB*, *ATP8*, *ATP9*, and *ATP6*. Semiquantitative PCR with a 40-cycle extension was used to detect *COX1-ATP8/ATP6*. Primers used are listed in Table S2. For clarity, agarose gel images shown in the figures were color inverted, resulting in dark bands on a white background.

Analysis of mitochondrial protein synthesis. Cells were grown in SD, SGal, or SG lacking methionine and cysteine to an OD_{600} of 1 at the indicated temperature as described in figures and figure legends of 23°C or 30°C or upon shift to 37°C from 23°C for the indicated time as described in figures and figure legends. Newly synthesized mitochondrial proteins were labeled with 0.1 mCi of ^{35}S-labeled methionine and cysteine (EasyTag Express^{35}S protein labeling mix; Perkin Elmer NEG77200 [specific activity, 1,175 Ci/mmol]) in the presence of cycloheximide for 30 min as described previously (107) at the indicated temperature of 23°C, 30°C, or 37°C. Mitochondria were isolated from labeled cells as described previously (107). Mitochondrial proteins were quantified by the Bradford assay, and equivalent amounts of protein were separated on a 17.5% SDS-PAGE gel. Labeled proteins were transferred to a nitrocellulose membrane and analyzed by a Fla9000 phosphorimager, or the gels were dried and exposed to X-ray film to visualize labeled proteins. Coomassie blue-stained gels were used as a part of normalization of radiolabeled mitochondrial proteins.

Immunoblot analysis. Proteins were separated on 7.5% or 10% SDS-PAGE gels and subjected to immunoblot analysis. The following antibodies were used: anti-Myc (1:5,000) (MYC.A7; Epitope Biotech, Inc.), Mrp7 (1:2,000) (108), Mrp13 (1:2,000) (109), Arg8p (21), and Mtg2 (49).

SUPPLEMENTAL MATERIAL

Supplemental material is available online only.

SUPPLEMENTAL FILE 1, PDF file, 1.2 MB.

ACKNOWLEDGMENTS

We are extremely grateful to Janine R. Maddock for strains, plasmids, and antibodies, Thomas D. Fox for antibodies to Arg8, Xochitl Pérez Martínez for strains YC162, RGV139, RGV140, and XPM78a, and Antoni Barrientos for strains XPM171a and W303I^0. We also thank Jagreet Kaur and Suman Dhar for critically reading the manuscript and Shahnaz Ansari for technical assistance. We are grateful for the instrumentation facilities at CIF, UDSC, and DST-FIST/UGC-SAP-supported CIF, Genetics.

This work was supported by grants from the Department of Biotechnology (grant no. BT/PR14740/BRB/10/875/2010 and BT/PR15104/GBD/27315/2011), SERB (grant no. EMR/2015/000650), and CSIR [grant no. 27(0324)/EMR-II] and by an R&D grant from Delhi University to K.D. and DU-IOE. J.K. acknowledges UGC, BSR, SERB, and ICMR for junior research fellowships and senior research fellowships.

J.K. performed experiments and analyzed data. K.D. and J.K. conceived the project, designed experiments, analyzed the data, and wrote the paper. K.D. was responsible for securing funding for this work.

REFERENCES

1. Stotland A, Gottlieb RA. 2015. Mitochondrial quality control: easy come, easy go. Biochim Biophys Acta 1853:2802–2811. https://doi.org/10.1016/j.bbamcr.2014.12.041.
2. Rutter J, Hughes AL. 2015. Power2: the power of yeast genetics applied to the powerhouse of the cell. Trends Endocrinol Metab 26:59–68. https://doi.org/10.1016/j.tem.2014.12.002.
3. Scheper GC, van der Knaap MS, Proud CG. 2007. Translation matters: protein synthesis defects in inherited disease. Nat Rev Genet 8:711–723. https://doi.org/10.1038/nrg2142.
4. Fox TD. 2012. Mitochondrial protein synthesis, import, and assembly. Genetics 192:1203–1234. https://doi.org/10.1534/genetics.112.141267.
5. Nagata S, Tsunetsugu-Yokota Y, Naito A, Kaziro Y. 1983. Molecular cloning and sequence determination of the nuclear gene coding for mitochondrial elongation factor Tu of Saccharomyces cerevisiae. Proc Natl Acad Sci U S A 80:6192–6196. https://doi.org/10.1073/pnas.80.20.6192.
6. Rasmussen SW. 1995. A 37.5 kb region of yeast chromosome X includes the SME1, MEF2, GSH1 and CSD3 genes, a TCP-1-related gene, an open reading frame similar to the DAL80 gene, and a tRNA(Arg). Yeast 11:873–883. https://doi.org/10.1002/yea.320110909.
7. Rosenthal LP, Bodley JW. 1987. Purification and characterization of Saccharomyces cerevisiae mitochondrial elongation factor Tu. J Biol Chem 262:10955–10959. https://doi.org/10.1016/S0021-9258(18)60910-X.
8. Vambutas A, Ackerman SH, Tzagoloff A. 1991. Mitochondrial translational-initiation and elongation factors in Saccharomyces cerevisiae. Eur J Biochem 201:643–652. https://doi.org/10.1111/j.1432-1033.1991.tb16325.x.
9. Costanzo MC, Bonnefoy N, Williams EH, Clark-Walker GD, Fox TD. 2000. Highly diverged homologs of Saccharomyces cerevisiae mitochondrial mRNA-specific translational activators have orthologous functions in other budding yeasts. Genetics 154:999–1012. https://doi.org/10.1093/genetics/154.3.999.
10. Ott M, Amunts A, Brown A. 2016. Organization and regulation of mitochondrial protein synthesis. Annu Rev Biochem 85:77–101. https://doi.org/10.1146/annurev-biochem-060815-014334.
11. Towpik J. 2005. Regulation of mitochondrial translation in yeast. Cell Mol Biol Lett 10:571–594.

12. Brown NG, Costanzo MC, Fox TD. 1994. Interactions among three proteins that specifically activate translation of the mitochondrial COX3 mRNA in Saccharomyces cerevisiae. Mol Cell Biol 14:1045–1053. https://doi.org/10.1128/mcb.14.2.1045-1053.1994.
13. Costanzo MC, Fox TD. 1993. Suppression of a defect in the 5' untranslated leader of mitochondrial COX3 mRNA by a mutation affecting an mRNA-specific translational activator protein. Mol Cell Biol 13:4806–4813. https://doi.org/10.1128/mcb.13.8.4806-4813.1993.
14. Green-Willms NS, Fox TD, Costanzo MC. 1998. Functional interactions between yeast mitochondrial ribosomes and mRNA 5' untranslated leaders. Mol Cell Biol 18:1826–1834. https://doi.org/10.1128/MCB.18.4.1826.
15. Dunstan HM, Green-Willms NS, Fox TD. 1997. In vivo analysis of Saccharomyces cerevisiae COX2 mRNA 5'-untranslated leader functions in mitochondrial translation initiation and translational activation. Genetics 147:87–100. https://doi.org/10.1093/genetics/147.1.87.
16. Haffter P, McMullin TW, Fox TD. 1991. Functional interactions among two yeast mitochondrial ribosomal proteins and an mRNA-specific translational activator. Genetics 127:319–326. https://doi.org/10.1093/genetics/127.2.319.
17. Naithani S, Saracco SA, Butler CA, Fox TD. 2003. Interactions among COX1, COX2, and COX3 mRNA-specific translational activator proteins on the inner surface of the mitochondrial inner membrane of Saccharomyces cerevisiae. Mol Biol Cell 14:324–333. https://doi.org/10.1091/mbc.e02-08-0490.
18. Lipinski KA, Kaniak-Golik A, Golik P. 2010. Maintenance and expression of the S. cerevisiae mitochondrial genome—from genetics to evolution and systems biology. Biochim Biophys Acta 1797:1086–1098. https://doi.org/10.1016/j.bbabio.2009.12.019.
19. Herrmann JM, Woellhaf MW, Bonnefoy N. 2013. Control of protein synthesis in yeast mitochondria: the concept of translational activators. Biochim Biophys Acta 1833:286–294. https://doi.org/10.1016/j.bbamcr.2012.03.007.
20. Kummer E, Ban N. 2021. Mechanisms and regulation of protein synthesis in mitochondria. Nat Rev Mol Cell Biol 22:307–325. https://doi.org/10.1038/s41580-021-00332-2.
21. Steele DF, Butler CA, Fox TD. 1996. Expression of a recoded nuclear gene inserted into yeast mitochondrial DNA is limited by mRNA-specific translational activation. Proc Natl Acad Sci U S A 93:5253–5257. https://doi.org/10.1073/pnas.93.11.5253.
22. Couvillion MT, Soto IC, Shipkovenska G, Churchman LS. 2016. Synchronized mitochondrial and cytosolic translation programs. Nature 533:499–503. https://doi.org/10.1038/nature18015.
23. Morgenstern M, Stiller SB, Lübbert P, Peikert CD, Dannenmaier S, Drepper F, Weill U, Höß P, Feuerstein R, Gebert M, Bohnert M, van der Laan M, Schuldiner M, Schütze C, Oeljeklaus S, Pfanner N, Wiedemann N, Warscheid B. 2017. Definition of a high-confidence mitochondrial proteome at quantitative scale. Cell Rep 19:2836–2852. https://doi.org/10.1016/j.celrep.2017.06.014.
24. Manthey GM, McEwen JE. 1995. The product of the nuclear gene PET309 is required for translation of mature mRNA and stability or production of intron-containing RNAs derived from the mitochondrial COX1 locus of Saccharomyces cerevisiae. EMBO J 14:4031–4043. https://doi.org/10.1002/j.1460-2075.1995.tb00074.x.
25. Zamudio-Ochoa A, Camacho-Villasana Y, Garcia-Guerrero AE, Perez-Martinez X. 2014. The Pet309 pentatricopeptide repeat motifs mediate efficient binding to the mitochondrial COX1 transcript in yeast. RNA Biol 11:953–967. https://doi.org/10.4161/rna.29780.
26. Barrientos A, Zambrano A, Tzagoloff A. 2004. Mss51p and Cox14p jointly regulate mitochondrial Cox1p expression in Saccharomyces cerevisiae. EMBO J 23:3472–3482. https://doi.org/10.1038/sj.emboj.7600358.
27. Perez-Martinez X, Broadley SA, Fox TD. 2003. Mss51p promotes mitochondrial Cox1p synthesis and interacts with newly synthesized Cox1p. EMBO J 22:5951–5961. https://doi.org/10.1093/emboj/cdg566.
28. Perez-Martinez X, Butler CA, Shingu-Vazquez M, Fox TD. 2009. Dual functions of Mss51 couple synthesis of Cox1 to assembly of cytochrome c oxidase in Saccharomyces cerevisiae mitochondria. Mol Biol Cell 20:4371–4380. https://doi.org/10.1091/mbc.e09-06-0522.
29. Roloff GA, Henry MF. 2015. Mam33 promotes cytochrome c oxidase subunit I translation in Saccharomyces cerevisiae mitochondria. Mol Biol Cell 26:2885–2894. https://doi.org/10.1091/mbc.E15-04-0222.
30. Szczesny RJ, Wojcik MA, Borowski LS, Szewczyk MJ, Skrok MM, Golik P, Stepien PP. 2013. Yeast and human mitochondrial helicases. Biochim Biophys Acta 1829:842–853. https://doi.org/10.1016/j.bbagrm.2013.02.009.
31. Jankowsky E, Fairman ME. 2007. RNA helicases—one fold for many functions. Curr Opin Struct Biol 17:316–324. https://doi.org/10.1016/j.sbi.2007.05.007.
32. Bourgeois CF, Mortreux F, Auboeuf D. 2016. The multiple functions of RNA helicases as drivers and regulators of gene expression. Nat Rev Mol Cell Biol 17:426–438. https://doi.org/10.1038/nrm.2016.50.
33. Jarmoskaite I, Russell R. 2014. RNA helicase proteins as chaperones and remodelers. Annu Rev Biochem 83:697–725. https://doi.org/10.1146/annurev-biochem-060713-035546.
34. Chen Y, Potratz JP, Tijerina P, Del Campo M, Lambowitz AM, Russell R. 2008. DEAD-box proteins can completely separate an RNA duplex using a single ATP. Proc Natl Acad Sci U S A 105:20203–20208. https://doi.org/10.1073/pnas.0811075106.
35. Henn A, Cao W, Licciardello N, Heitkamp SE, Hackney DD, De La Cruz EM. 2010. Pathway of ATP utilization and duplex rRNA unwinding by the DEAD-box helicase, DbpA. Proc Natl Acad Sci U S A 107:4046–4050. https://doi.org/10.1073/pnas.0913081107.
36. Henn A, Bradley MJ, De La Cruz EM. 2012. ATP utilization and RNA conformational rearrangement by DEAD-box proteins. Annu Rev Biophys 41:247–267. https://doi.org/10.1146/annurev-biophys-050511-102243.
37. Fairman ME, Maroney PA, Wang W, Bowers HA, Gollnick P, Nilsen TW, Jankowsky E. 2004. Protein displacement by DExH/D "RNA helicases" without duplex unwinding. Science 304:730–734. https://doi.org/10.1126/science.1095596.
38. Linder P, Jankowsky E. 2011. From unwinding to clamping—the DEAD box RNA helicase family. Nat Rev Mol Cell Biol 12:505–516. https://doi.org/10.1038/nrm3154.
39. De Silva D, Poliquin S, Zeng R, Zamudio-Ochoa A, Marrero N, Perez-Martinez X, Fontanesi F, Barrientos A. 2017. The DEAD-box helicase Mss116 plays distinct roles in mitochondrial ribogenesis and mRNA-specific translation. Nucleic Acids Res 45:6628–6643. https://doi.org/10.1093/nar/gkx426.
40. Halls C, Mohr S, Del Campo M, Yang Q, Jankowsky E, Lambowitz AM. 2007. Involvement of DEAD-box proteins in group I and group II intron splicing. Biochemical characterization of Mss116p, ATP hydrolysis-dependent and -independent mechanisms, and general RNA chaperone activity. J Mol Biol 365:835–855. https://doi.org/10.1016/j.jmb.2006.09.083.
41. Markov DA, Wojtas ID, Tessitore K, Henderson S, McAllister WT. 2014. Yeast DEAD box protein Mss116p is a transcription elongation factor that modulates the activity of mitochondrial RNA polymerase. Mol Cell Biol 34:2360–2369. https://doi.org/10.1128/MCB.00160-14.
42. Zingler N, Solem A, Pyle AM. 2010. Dual roles for the Mss116 cofactor during splicing of the ai5gamma group II intron. Nucleic Acids Res 38:6602–6609. https://doi.org/10.1093/nar/gkq530.
43. De Silva D, Fontanesi F, Barrientos A. 2013. The DEAD box protein Mrh4 functions in the assembly of the mitochondrial large ribosomal subunit. Cell Metab 18:712–725. https://doi.org/10.1016/j.cmet.2013.10.007.
44. Dziembowski A, Piwowarski J, Hoser R, Minczuk M, Dmochowska A, Siep M, van der Spek H, Grivell L, Stepien PP. 2003. The yeast mitochondrial degradosome. Its composition, interplay between RNA helicase and RNase activities and the role in mitochondrial RNA metabolism. J Biol Chem 278:1603–1611. https://doi.org/10.1074/jbc.M208287200.
45. Malecki M, Jedrzejczak R, Stepien PP, Golik P. 2007. In vitro reconstitution and characterization of the yeast mitochondrial degradosome complex unravels tight functional interdependence. J Mol Biol 372:23–36. https://doi.org/10.1016/j.jmb.2007.06.074.
46. Turk EM, Caprara MG. 2010. Splicing of yeast al5beta group I intron requires SUV3 to recycle MRS1 via mitochondrial degradosome-promoted decay of excised intron ribonucleoprotein (RNP). J Biol Chem 285:8585–8594. https://doi.org/10.1074/jbc.M109.090761.
47. Sedman T, Gaidutsik I, Villemson K, Hou Y, Sedman J. 2014. Double-stranded DNA-dependent ATPase Irc3p is directly involved in mitochondrial genome maintenance. Nucleic Acids Res 42:13214–13227. https://doi.org/10.1093/nar/gku1148.
48. Piljukov VJ, Garber N, Sedman T, Sedman J. 2020. Irc3 is a monomeric DNA branch point-binding helicase in mitochondria of the yeast Saccharomyces cerevisiae. FEBS Lett 594:3142–3155. https://doi.org/10.1002/1873-3468.13893.
49. Datta K, Fuentes JL, Maddock JR. 2005. The yeast GTPase Mtg2p is required for mitochondrial translation and partially suppresses an rRNA methyltransferase mutant, mrm2. Mol Biol Cell 16:954–963. https://doi.org/10.1091/mbc.e04-07-0622.
50. Myers AM, Pape LK, Tzagoloff A. 1985. Mitochondrial protein synthesis is required for maintenance of intact mitochondrial genomes in Saccharomyces cerevisiae. EMBO J 4:2087–2092. https://doi.org/10.1002/j.1460-2075.1985.tb03896.x.

51. Fairman-Williams ME, Guenther UP, Jankowsky E. 2010. SF1 and SF2 helicases: family matters. Curr Opin Struct Biol 20:313–324. https://doi.org/10.1016/j.sbi.2010.03.011.
52. Cordin O, Banroques J, Tanner NK, Linder P. 2006. The DEAD-box protein family of RNA helicases. Gene 367:17–37. https://doi.org/10.1016/j.gene.2005.10.019.
53. Ellis TP, Helfenbein KG, Tzagoloff A, Dieckmann CL. 2004. Aep3p stabilizes the mitochondrial bicistronic mRNA encoding subunits 6 and 8 of the H^+-translocating ATP synthase of Saccharomyces cerevisiae. J Biol Chem 279:15728–15733. https://doi.org/10.1074/jbc.M314162200.
54. Pelissier PP, Camougrand NM, Manon ST, Velours GM, Guerin MG. 1992. Regulation by nuclear genes of the mitochondrial synthesis of subunits 6 and 8 of the ATP synthase of Saccharomyces cerevisiae. J Biol Chem 267:2467–2473. https://doi.org/10.1016/S0021-9258(18)45902-9.
55. Scheffler IE, de la Cruz BJ, Prieto S. 1998. Control of mRNA turnover as a mechanism of glucose repression in Saccharomyces cerevisiae. Int J Biochem Cell Biol 30:1175–1193. https://doi.org/10.1016/s1357-2725(98)00086-7.
56. Conrad M, Schothorst J, Kankipati HN, Van Zeebroeck G, Rubio-Texeira M, Thevelein JM. 2014. Nutrient sensing and signaling in the yeast Saccharomyces cerevisiae. FEMS Microbiol Rev 38:254–299. https://doi.org/10.1111/1574-6976.12065.
57. Johnston M. 1999. Feasting, fasting and fermenting. Glucose sensing in yeast and other cells. Trends Genet 15:29–33. https://doi.org/10.1016/s0168-9525(98)01637-0.
58. Kehrein K, Schilling R, Moller-Hergt BV, Wurm CA, Jakobs S, Lamkemeyer T, Langer T, Ott M. 2015. Organization of mitochondrial gene expression in two distinct ribosome-containing assemblies. Cell Rep 10:843–853. https://doi.org/10.1016/j.celrep.2015.01.012.
59. Fontanesi F, Soto IC, Horn D, Barrientos A. 2006. Assembly of mitochondrial cytochrome c-oxidase, a complicated and highly regulated cellular process. Am J Physiol Cell Physiol 291:C1129–47. https://doi.org/10.1152/ajpcell.00233.2006.
60. Singh AP, Salvatori R, Aftab W, Aufschnaiter A, Carlstrom A, Forne I, Imhof A, Ott M. 2020. Molecular connectivity of mitochondrial gene expression and OXPHOS biogenesis. Mol Cell 79:1051–1065.e10. https://doi.org/10.1016/j.molcel.2020.07.024.
61. Rodeheffer MS, Boone BE, Bryan AC, Shadel GS. 2001. Nam1p, a protein involved in RNA processing and translation, is coupled to transcription through an interaction with yeast mitochondrial RNA polymerase. J Biol Chem 276:8616–8622. https://doi.org/10.1074/jbc.M009901200.
62. Mays JN, Camacho-Villasana Y, Garcia-Villegas R, Perez-Martinez X, Barrientos A, Fontanesi F. 2019. The mitoribosome-specific protein mS38 is preferentially required for synthesis of cytochrome c oxidase subunits. Nucleic Acids Res 47:5746–5760. https://doi.org/10.1093/nar/gkz266.
63. Sesaki H, Jensen RE. 2001. UGO1 encodes an outer membrane protein required for mitochondrial fusion. J Cell Biol 152:1123–1134. https://doi.org/10.1083/jcb.152.6.1123.
64. Buglino J, Shen V, Hakimian P, Lima CD. 2002. Structural and biochemical analysis of the Obg GTP binding protein. Structure 10:1581–1592. https://doi.org/10.1016/s0969-2126(02)00882-1.
65. Dever TE, Kinzy TG, Pavitt GD. 2016. Mechanism and regulation of protein synthesis in Saccharomyces cerevisiae. Genetics 203:65–107. https://doi.org/10.1534/genetics.115.186221.
66. Turcotte B, Liang XB, Robert F, Soontorngun N. 2010. Transcriptional regulation of nonfermentable carbon utilization in budding yeast. FEMS Yeast Res 10:2–13. https://doi.org/10.1111/j.1567-1364.2009.00555.x.
67. DeRisi JL, Iyer VR, Brown PO. 1997. Exploring the metabolic and genetic control of gene expression on a genomic scale. Science 278:680–686. https://doi.org/10.1126/science.278.5338.680.
68. Gasch AP, Spellman PT, Kao CM, Carmel-Harel O, Eisen MB, Storz G, Botstein D, Brown PO. 2000. Genomic expression programs in the response of yeast cells to environmental changes. Mol Biol Cell 11:4241–4257. https://doi.org/10.1091/mbc.11.12.4241.
69. Brauer MJ, Huttenhower C, Airoldi EM, Rosenstein R, Matese JC, Gresham D, Boer VM, Troyanskaya OG, Botstein D. 2008. Coordination of growth rate, cell cycle, stress response, and metabolic activity in yeast. Mol Biol Cell 19:352–367. https://doi.org/10.1091/mbc.e07-08-0779.
70. Paulo JA, O'Connell JD, Gaun A, Gygi SP. 2015. Proteome-wide quantitative multiplexed profiling of protein expression: carbon-source dependency in Saccharomyces cerevisiae. Mol Biol Cell 26:4063–4074. https://doi.org/10.1091/mbc.E15-07-0499.
71. Takeda M. 1981. Glucose-induced inactivation of mitochondrial enzymes in the yeast Saccharomyces cerevisiae. Biochem J 198:281–287. https://doi.org/10.1042/bj1980281.
72. Bouchez CL, Hammad N, Cuvellier S, Ransac S, Rigoulet M, Devin A. 2020. The Warburg effect in yeast: repression of mitochondrial metabolism is not a prerequisite to promote cell proliferation. Front Oncol 10:1333. https://doi.org/10.3389/fonc.2020.01333.
73. Ohlmeier S, Kastaniotis AJ, Hiltunen JK, Bergmann U. 2004. The yeast mitochondrial proteome, a study of fermentative and respiratory growth. J Biol Chem 279:3956–3979. https://doi.org/10.1074/jbc.M310160200.
74. Khong A, Parker R. 2020. The landscape of eukaryotic mRNPs. RNA 26:229–239. https://doi.org/10.1261/rna.073601.119.
75. Mortimer SA, Kidwell MA, Doudna JA. 2014. Insights into RNA structure and function from genome-wide studies. Nat Rev Genet 15:469–479. https://doi.org/10.1038/nrg3681.
76. Jacobs E, Mills JD, Janitz M. 2012. The role of RNA structure in posttranscriptional regulation of gene expression. J Genet Genomics 39:535–543. https://doi.org/10.1016/j.jgg.2012.08.002.
77. Mauger DM, Siegfried NA, Weeks KM. 2013. The genetic code as expressed through relationships between mRNA structure and protein function. FEBS Lett 587:1180–1188. https://doi.org/10.1016/j.febslet.2013.03.002.
78. Khong A, Matheny T, Jain S, Mitchell SF, Wheeler JR, Parker R. 2017. The stress granule transcriptome reveals principles of mRNA accumulation in stress granules. Mol Cell 68:808–820.e5. https://doi.org/10.1016/j.molcel.2017.10.015.
79. Yu H, Meng W, Mao Y, Zhang Y, Sun Q, Tao S. 2019. Deciphering the rules of mRNA structure differentiation in Saccharomyces cerevisiae in vivo and in vitro with deep neural networks. RNA Biol 16:1044–1054. https://doi.org/10.1080/15476286.2019.1612692.
80. Adivarahan S, Livingston N, Nicholson B, Rahman S, Wu B, Rissland OS, Zenklusen D. 2018. Spatial organization of single mRNPs at different stages of the gene expression pathway. Mol Cell 72:727–738 e5. https://doi.org/10.1016/j.molcel.2018.10.010.
81. Amiott EA, Jaehning JA. 2006. Mitochondrial transcription is regulated via an ATP "sensing" mechanism that couples RNA abundance to respiration. Mol Cell 22:329–338. https://doi.org/10.1016/j.molcel.2006.03.031.
82. Gaidutsik I, Sedman T, Sillamaa S, Sedman J. 2016. Irc3 is a mitochondrial DNA branch migration enzyme. Sci Rep 6:26414. https://doi.org/10.1038/srep26414.
83. Guo XE, Chen CF, Wang DD, Modrek AS, Phan VH, Lee WH, Chen PL. 2011. Uncoupling the roles of the SUV3 helicase in maintenance of mitochondrial genome stability and RNA degradation. J Biol Chem 286:38783–38794. https://doi.org/10.1074/jbc.M111.257956.
84. Shu Z, Vijayakumar S, Chen CF, Chen PL, Lee WH. 2004. Purified human SUV3p exhibits multiple-substrate unwinding activity upon conformational change. Biochemistry 43:4781–4790. https://doi.org/10.1021/bi0356449.
85. Tuteja N, Tarique M, Tuteja R. 2014. Rice SUV3 is a bidirectional helicase that binds both DNA and RNA. BMC Plant Biol 14:283. https://doi.org/10.1186/s12870-014-0283-6.
86. Datta K, Skidmore JM, Pu K, Maddock JR. 2004. The Caulobacter crescentus GTPase CgtAC is required for progression through the cell cycle and for maintaining 50S ribosomal subunit levels. Mol Microbiol 54:1379–1392. https://doi.org/10.1111/j.1365-2958.2004.04354.x.
87. Jiang M, Datta K, Walker A, Strahler J, Bagamasbad P, Andrews PC, Maddock JR. 2006. The Escherichia coli GTPase CgtAE is involved in late steps of large ribosome assembly. J Bacteriol 188:6757–6770. https://doi.org/10.1128/JB.00444-06.
88. Kint C, Verstraeten N, Hofkens J, Fauvart M, Michiels J. 2014. Bacterial Obg proteins: GTPases at the nexus of protein and DNA synthesis. Crit Rev Microbiol 40:207–224. https://doi.org/10.3109/1040841X.2013.776510.
89. Dutkiewicz R, Slomińska M, Wegrzyn G, Czyz A. 2002. Overexpression of the cgtA (yhbZ, obgE) gene, coding for an essential GTP-binding protein, impairs the regulation of chromosomal functions in Escherichia coli. Curr Microbiol 45:440–445. https://doi.org/10.1007/s00284-002-3713-x.
90. Sikora AE, Zielke R, Wegrzyn A, Wegrzyn G. 2006. DNA replication defect in the Escherichia coli cgtA(ts) mutant arising from reduced DnaA levels. Arch Microbiol 185:340–347. https://doi.org/10.1007/s00203-006-0099-3.
91. Foti JJ, Schienda J, Sutera VA, Jr, Lovett ST. 2005. A bacterial G protein-mediated response to replication arrest. Mol Cell 17:549–560. https://doi.org/10.1016/j.molcel.2005.01.012.
92. Kallstrom G, Hedges J, Johnson A. 2003. The putative GTPases Nog1p and Lsg1p are required for 60S ribosomal subunit biogenesis and are localized to the nucleus and cytoplasm, respectively. Mol Cell Biol 23:4344–4355. https://doi.org/10.1128/MCB.23.12.4344-4355.2003.
93. Saveanu C, Namane A, Gleizes PE, Lebreton A, Rousselle JC, Noaillac-Depeyre J, Gas N, Jacquier A, Fromont-Racine M. 2003. Sequential protein association with nascent 60S ribosomal particles. Mol Cell Biol 23:4449–4460. https://doi.org/10.1128/MCB.23.13.4449-4460.2003.

94. Du YC, Stillman B. 2002. Yph1p, an ORC-interacting protein: potential links between cell proliferation control, DNA replication, and ribosome biogenesis. Cell 109:835–848. https://doi.org/10.1016/s0092-8674(02)00773-0.
95. Berthon J, Fujikane R, Forterre P. 2009. When DNA replication and protein synthesis come together. Trends Biochem Sci 34:429–434. https://doi.org/10.1016/j.tibs.2009.05.004.
96. Prigione A, Ruiz-Perez MV, Bukowiecki R, Adjaye J. 2015. Metabolic restructuring and cell fate conversion. Cell Mol Life Sci 72:1759–1777. https://doi.org/10.1007/s00018-015-1834-1.
97. Xu X, Duan S, Yi F, Ocampo A, Liu GH, Izpisua Belmonte JC. 2013. Mitochondrial regulation in pluripotent stem cells. Cell Metab 18:325–332. https://doi.org/10.1016/j.cmet.2013.06.005.
98. Vander Heiden MG, Cantley LC, Thompson CB. 2009. Understanding the Warburg effect: the metabolic requirements of cell proliferation. Science 324:1029–1033. https://doi.org/10.1126/science.1160809.
99. Diaz-Ruiz R, Rigoulet M, Devin A. 2011. The Warburg and Crabtree effects: on the origin of cancer cell energy metabolism and of yeast glucose repression. Biochim Biophys Acta 1807:568–576. https://doi.org/10.1016/j.bbabio.2010.08.010.
100. Diaz-Ruiz R, Uribe-Carvajal S, Devin A, Rigoulet M. 2009. Tumor cell energy metabolism and its common features with yeast metabolism. Biochim Biophys Acta 1796:252–265. https://doi.org/10.1016/j.bbcan.2009.07.003.
101. Claros MG, Vincens P. 1996. Computational method to predict mitochondrially imported proteins and their targeting sequences. Eur J Biochem 241:779–786. https://doi.org/10.1111/j.1432-1033.1996.00779.x.
102. Guthrie C, Fink GR. 1991. Guide to yeast genetics and molecular biology. Methods Enzymol 194:1–863.
103. Longtine MS, McKenzie A, III, Demarini DJ, Shah NG, Wach A, Brachat A, Philippsen P, Pringle JR. 1998. Additional modules for versatile and economical PCR-based gene deletion and modification in Saccharomyces cerevisiae. Yeast 14:953–961. https://doi.org/10.1002/(SICI)1097-0061(199807)14:10<953::AID-YEA293>3.0.CO;2-U.
104. Stark MJR. 1998. Studying essential genes: generating and using promoter fusions and conditional alleles. Yeast Gene Analysis 26:83–99. https://doi.org/10.1016/S0580-9517(08)70327-1.
105. Glick BS, Pon LA. 1995. Isolation of highly purified mitochondria from Saccharomyces cerevisiae. Methods Enzymol 260:213–223. https://doi.org/10.1016/0076-6879(95)60139-2.
106. Fearon K, Mason TL. 1992. Structure and function of MRP20 and MRP49, the nuclear genes for two proteins of the 54 S subunit of the yeast mitochondrial ribosome. J Biol Chem 267:5162–5170. https://doi.org/10.1016/S0021-9258(18)42745-7.
107. Fox TD, Folley LS, Mulero JJ, McMullin TW, Thorsness PE, Hedin LO, Costanzo MC. 1991. Analysis and manipulation of yeast mitochondrial genes. Methods Enzymol 194:149–165. https://doi.org/10.1016/0076-6879(91)94013-3.
108. Fearon K, Mason TL. 1988. Structure and regulation of a nuclear gene in Saccharomyces cerevisiae that specifies MRP7, a protein of the large subunit of the mitochondrial ribosome. Mol Cell Biol 8:3636–3646. https://doi.org/10.1128/mcb.8.9.3636-3646.1988.
109. Partaledis JA, Mason TL. 1988. Structure and regulation of a nuclear gene in Saccharomyces cerevisiae that specifies MRP13, a protein of the small subunit of the mitochondrial ribosome. Mol Cell Biol 8:3647–3660. https://doi.org/10.1128/mcb.8.9.3647-3660.1988.